In presenting the dissertation as a partial fulfillment of the requirements for an advanced degree from the Georgia Institute of Technology, I agree that the Library of the Institute shall make it available for inspection and circulation in accordance with its regulations governing materials of this type. I agree that permission to copy from, or to publish from, this dissertation may be granted by the professor under whose direction it was written, or, in his absence, by the Dean of the Graduate Division when such copying or publication is solely for scholarly purposes and does not involve potential financial gain. It is understood that any copying from, or publication of, this dissertation which involves potential financial gain will not be allowed without written permission.

3/17/65
b

BEARING CAPACITY OF A CLOSED JOINTED ROCK

A THESIS

Presented to

The Faculty of the Graduate Division

by

Banwari Lal Bishnoi

In Partial Fulfillment

of the Requirements for the Degree

Doctor of Philosophy

in the School of Civil Engineering

Georgia Institute of Technology

June, 1968

BEARING CAPACITY OF A CLOSED

JOINTED ROCK

Approved:

Chairman

Date approved by Chairman: June 2, 1968

Dedication

To the memory of my father

ACKNOWLEDGMENTS

The author wishes to express his deep gratitude to Professor G. F. Sowers for his advice, guidance and instruction of this study.

Special thanks are also extended to Dr. B. B. Mazanti and Dr. J. H. Armstrong for their special interest, help, and the efforts expended in the evaluation of the investigation, as well as to Mr. K. D. Bishnoi, Mr. Raymond Andrews, and S. P. Agarwal for their continuing encouragement during the work.

TABLE OF CONTENTS

TABLE OF CONTENTS (Continued)

LIST OF TABLES

LIST OF TABLES (Continued)

LIST OF ILLUSTRATIONS

LIST OF ILLUSTRATIONS (Continued)

LIST OF SYMBOLS

Symbol

- α - semi wedge angle $(45 - \varphi/2)$
- c - cohesion of the material
- φ - angle of internal friction
- q_o - ultimate bearing capacity of soil or rock
- Q - failure load
- q_c - ultimate bearing capacity of circular footings
- q_s - ultimate bearing capacity of strip footings
- q_{sq} - ultimate bearing capacity of square footings
- p_t - tensile strength of material
- p_h - horizontal splitting pressure
- p_o - confining pressure for the closed jointed system
- B - footing width
- L - width of the individual block
- H - height of the individual block
- N_φ - $\tan^2 (45 + \varphi/2)$
- R_c - rock bearing capacity factor
- R_p - rock bearing capacity factor
- J - modification factor for footings for case of $\frac{H}{B} \leq 8$
- S - shape factor for strip footings
- N_c, N_r - general bearing capacity factors

CHAPTER I

INTRODUCTION

Statement of the Problem

The bearing capacity of soil or rock is one of the main problems in the design of foundations for large structures. The maximum pressure which the ground can sustain without failure is its ultimate bearing capacity (26). Within this limit the foundation pressure should be further limited so that the settlement of the structure and the resulting secondary stresses in its members are not excessive.

A summary of the existing knowledge of the bearing capacity of the rock showed that there has been very little research work in the past concerned with the bearing capacity of rock. The reason seems to be that in the past the loads placed on foundation rock have been of such a small magnitude, that it was taken for granted that the structure would be safe. It appears that new situations are developing in which the stability of the foundation-rock system becomes a matter of concern. Increasingly heavy structural loads, small diameter cassions, and, such projects as space vehicle launchers, which develop very high loads on the foundations, emphasize the importance and limitation of rock as a foundation material. The importance of the effect of stresses and deformational characteristics of rock mass became more important with opening deeper and deeper holes for search of important materials and tectonic investigations. The bearing capacity of the rock is critical for very high dams built on rock foundations.

Much of the theoretical information available on bearing capacity of rock do not substantiate the experimental results and thus cannot be used for practical purposes.

The important factors in bearing capacity are governed by the mechanical properties of the material (density, shearing strength and deformational characteristics), on the stresses in the ground before the foundation is constructed, on the physical characteristics of the foundation, including the shape and the stiffness and the nature of loads. Most of the research done on bearing capacity deals with an idealized semi-infinite medium, that is homogeneous and isotropic. As this is seldom the case in either soil or rock, particularly in rocks with joints, the need for more realistic analysis has increased in recent times.

It is realized that the technological properties of rock mass depend far more upon the system of geological separations within the mass than on the strength of the rock material itself (1). Therefore, rock mechanics is to be a mechanics of a discontinuum; that is, a jointed system. It is hypothesized by John (1) that the deformability or settlement expected from a rock mass results primarily from displacements of the unit blocks (the rock between a set of joints) and not from deformity of the block itself. In other words the macrogeological weaknesses such as joints, which would appear in a rock mass in practice are much more important than the intact rock mass. The earlier work by Meyerhof (2), Bach (11), Graf (12) was done on intact rock mass or concrete blocks without weaknesses such as joints which may appear in the field. This work has probably been so done because of the difficulties involved in simulating a jointed system.

Purpose of the Research

The purpose of this investigation was to evaluate the effects of joints and to develop a method of analysis which could be used to predict the bearing capacity from a knowledge of the rock, and the geometry, of the rock blocks and the jointed rock system. A regularly jointed rock system was simulated, and loading tests were performed on this system, using model footings. The objective was to determine the effects on the bearing capacity, due to the spacing of the joints. Using model footings tests were done on different sizes of rock blocks forming different jointed systems. The effects of the confinement by the adjoining blocks in a closed jointed rock system was evaluated by tests on rock blocks confined in a box. Different shapes and sizes of model footings were used for the purpose, to investigate the effect of footing geometry on the bearing capacity. It was recognized that an exhaustive study of the bearing capacity of a jointed rock system was beyond the scope of any single research project such as this and thus the shapes of model footings used and the number of different sizes of blocks used had to be limited. However, it is believed that variations chosen in this investigation for the shapes and sizes of rock blocks and model footings are sufficiently broad to form a comprehensive picture of the topic. Finally the investigation was extensive enough to obtain a general solution, which could be used for practical purposes, for similar rocks.

In this investigation the rock used was Indiana Limestone, chosen for the uniformity of the material and the ease with which this rock could be formed into blocks of desired size. The apparatus used, types of tests and the test procedures are described in Chapters III and IV. The results

of the model load tests are given in Chapter V. These results are used to analyze the failure characteristics and the bearing capacity, using the strength parameters, the cohesion and internal friction of the material.

This investigation considers only single vertical loads acting centrally on foundations with horizontal base. A semi-theoretical expression based on the theory of plasticity has been developed to calculate an approximate value of the bearing capacity of circular foundations, in terms of the confining stresses, geometry of the foundation and the rock blocks and the shearing characteristics of the material. Based on experimental data, for rectangular and square model footings emperical shape factors have been suggested. The results of the model tests seem to be in reasonable agreement with the theory developed in this study.

CHAPTER II

REVIEW OF LITERATURE

The maximum pressure which the ground can sustain without failure is its ultimate bearing capacity (26). Compression tests indicate that soil fails in shear. An estimate of its ability to support an applied load is made either by comparing the shear stresses induced by the foundation with the shear strength of the ground, or by assuming a rupture surface and analyzing the stability against shear failure of the material along this surface. There have been many different theories put forward by different writers for calculating the bearing capacity.

The classical earth pressure theory assumes that on exceeding a certain stress condition, rupture surfaces are formed in the soil mass. Thus, the footing pressure existing upon the formation of rupture surfaces, may be considered as the ultimate bearing capacity of the soil.

Based on the above assumption, the bearing capacity can be determined from the relation of the principal stresses which occur upon the formation of the rupture surfaces. The pertinent theories are those by Pauker (5), Rankine (6), Ritter (7), Bell (8). From the shape of the rupture surfaces, the bearing capacity can be determined. The principal forms of rupture surfaces used in engineering practice are: broken planes, circular, circular with a tangent, logarithmically spiralled, logarithmically spiralled with a tangent, and cycloids. The calculated

bearing capacity may be of different magnitude depending upon the shape of the assumed zone of failure.

One of the oldest formulas for the determination of soil bearing capacity and depth of laying of foundations is that given by Pauker (5). The principle of Pauker's theory is the equilibrium condition of a point within a mass. The formula is derived based on the classical earth pressure theory of an ideal non-cohesive material. Resistance to shear in the mass is therefore provided by frictional forces only and the weight of the structural load or the ultimate contact pressure is replaced by an equivalent height of material whose unit weight is the same as that of the material in which the foundation is laid. Pauker's formula is a simple one, but it has some limitations, as on ground surface by this formula the bearing capacity is zero. This contradicts the experimental results, because the material at the ground surface has some ability to support a load. This results from not including in the equation the unit weight of soil of the rupturing soil wedge below the footing. Also, Pauker's equation does not consider the width of the foundation.

Whatever deficiencies were inherent in the reasoning in Pauker's theory, they were compensated his recommending a factor of safety n, of 1.5 to 3.0, thus obtaining a safe bearing capacity of an ideal, granular material.

Ritter (7) gave another theory stating that when pressure on a footing causes failure of the material, a wedge is pushed into the ground, some of which is forced up at either side. For equilibrium against horizontal displacement Ritter determined the passive earth pressure thrusts on the wedge, and on the foundation face. Using Coulomb's wedge theory he

obtained an analytical expression for the bearing capacity. Ritter's theory gives low estimates as the equilibrium of only one half side of footing is considered without giving consideration to the whole system.

If the footing width is taken as zero in Ritter's expression, the expression derived by Bell (8) is obtained who determined the bearing capacity from the equilibrium of pressures at the foundation edge. If in addition the cohesion is zero, the above equation becomes identical to Rankine's (6) formula. This also leads to the unsatisfactory result of zero bearing capacity at the surface of cohesionless soil. The more conservative special cases of Bell and Rankine indicate that bearing capacity cannot reasonably be computed from the stability at the footing edge.

Prandtl (9) studied the process of penetration of hard bodies, such as metal punches, into softer, homogeneous, isotropic material from the point of view of plastic equilibrium. (Meyerhof (2) suggested that the Prandtl approach can be used for finding bearing capacity of semi-infinite, homogeneous rock mass or very large blocks of rock.) One of Prandtl's systems of study was a two-dimensional penetration problem in which a vertical punch of width, 2b and infinite length was applied to the horizontal surface of a semi-infinite body. The puncher reminds one of a surface strip loading of very long length perpendicular to the drawing plane. The contact surface between the punch and the other materials is assumed to be smooth.

In applying the theory of plasticity in his studies of plastic failure in metals, Prandtl followed the following line of reasoning. Because the elastic deformations with most common materials are very small,

Prandtl neglected them and using Airy's stress function obtained a differential equation of the second order, the solution of which gives the analytical expression for the ultimate punching (or bearing) stress, q_o.

The precision of Prandtl's equation for calculating the ultimate bearing capacity of soil depends very much upon the assumed shape of the rupture surface. The rupture surface curve is a compound one, and consists of arcs of a logarithmic spiral and a tangent to the spiral. This theory is used for a long strip foundation. When $c = o$ and $\varphi > 0$, then by Prandtl's original equation, $q_o = 0$. Thus the ultimate bearing capacity of an ideal, frictional material at its ground surface is zero, which is in contradiction to common observations in reality. The contradiction originates mainly from the assumption that the material is assumed to be weightless. With the introduced corrections, the bearing capacity of the soil has a real value > 0.

Based on Prandtl's theory of plastic failure Terzaghi (10) presented a modified system. If we think of a footing as being a limiting case of a wall rotated until it is horizontal with the ground surface, then the application of stresses to the footing develops passive pressures in the underlying soil. In the general case, we may deduce from the solution to the wall problem that the maximum stress which can be applied to the footing to cause yield in the soil or rock will have a finite value at the edge of the footing due to the presence of a surcharge. The stress will increase with distance from the edge of the footing, due to the effect of the materials weight. In general, the stress may no longer increase linearly with distance from the edge of the footing, and the constants associated with the surcharge and weight contributions will be different. If the material

also possesses some cohesion, then the maximum stress on the footing at yield will be increased by a constant amount in the same way that the surcharge requires a constant level of stress at limiting equilibrium, and we will need another coefficient to describe the effect of the presence of cohesion in the soil.

On this basis, Terzaghi observed that the ultimate normal load that could be applied to the surface could be approximately estimated by superposing the limit stresses obtained for weightless material whose ability to sustain a surface stress depends only on the presence of a surcharge and for material having weight, in the absence of a surcharge with material lacking weight, but possessing cohesion. Such a superposition method does not lead to a correct solution, but, in many cases, it enabled one to find an approximate answer without the labor involved in solving the problem by numerical methods.

Terzaghi's system is devised for a shallow strip footing ($D_f < 2b$), with its base at a distance of D_f below the ground surface. It was assumed that the ground surface at the base line of the footing is loaded with a uniformly distributed load $p = \gamma D_f$ and the soil or rock above the level of the base of the footing has no shearing resistance. The footing exerts on the material a pressure of q_o. The material wedge underneath the base of the footing is considered an elastic medium, and is assigned by Terzaghi a unit weight γ. The base of the footing is assumed to be rough. The critical load $Q_o = q_o(2b)$ on the soil is calculated based on the principle of static equilibrium of the soil wedge, supported laterally by passive earth pressure.

Terzaghi's method of analysis of bearing capacity of a cohesive

material shows that the ultimate bearing capacity of a purely cohesive material is independent of the width of footing.

The assumption that the depth of the footing below the surface can be represented simply as a surcharge stress over the surface at the footing level is a conservative one, giving rise to computed footing loads smaller than those which would actually be obtained from a more realistic approach that included the resistance to shearing of the soil above the failure zone. Meyerhof (3) has considered this problem and has computed approximately the bearing capacity factors for footings of all depths, based on the observed behavior of rough-based footings in tests. In his analysis Meyerhof uses a parameter β, the angle of the line drawn from the base of the footing to the point where the assumed bounding failure slip line intersects the soil surface. The β plane is termed the equivalent free surface. The wedge of soil between the plane and the side of the footing exerts a normal and a shearing stress on the equivalent free surface, which, in Meyerhof's analysis, take the place of the surcharge stress previously considered to be due to the weight of the soil above the base level of the footing.

From his calculations, Meyerhof obtained a diagram relating the bearing capacity factor N_q to the angle of internal friction and the equivalent free surface angle β, which represents the depth of the footing below the surface. The parameters N_q and N_γ do not vary much with the extent to which friction is assumed to act on the equivalent free surface.

The ratio of the depth of the footing to its breadth is also related to β and φ by an equation given by Meyerhof. To determine the bearing capacity of a footing in a given case, this diagram can be used to find β

and q_o for a given ratio of the depth of the footing to its breadth and φ. Meyerhof's results are close to Terzaghi's values at the surface, we can see that the contribution of the shearing resistance of soil above the base of the footing substantially increases the values of N_γ at shallow depths. For shallow footings the product $\gamma D_f N_q$ obtained by Meyerhof is virtually identical with the product $\gamma D_f N_q$ of Terzaghi.

Using the values obtained by Meyerhof for a strip footing with a rough base at or near the surface, we can see that for $\varphi = 30°$, $N_q/N_\gamma \approx 1$, and for $\varphi = 40°$, $N_q/N_\gamma \approx 0.6$. In model tests on footings, Meyerhof (3) found that the ratio of the two bearing capacity factors for a dense sand was 0.7, so that, in this case, the theoretical results appear to be confirmed.

Feda (4) also gives a relationship based on tests in which the ratio of N_q to N_γ is very close to unity, and Hansen (13) takes N_q to be equal to N_γ. It would appear that his equation closely expresses the ultimate bearing capacity of a rough footing on a cohesionless soil as a function of depth, up to depths approximately equal to the footing width.

The value of the factor N_c in terms of φ for a strip footing with a rough base was obtained by Terzaghi and also by Meyerhof. The values obtained by the two investigators are almost identical for a footing at the surface.

Analytical solutions from which one can derive the bearing capacities of different footings on or in materials of the general type have not been developed, although Sokolvski (14) arrived at a numerical solution. His method was employed by Hajal (15), who used a computer to obtain tables and graphs of solutions from which many general results of practical

interest can be calculated. Because of the number of variables, and the nonlinearity of the basic equations, any numerically obtained solution to, say, a surface loading condition, is valid only for the angle of friction of the material used in the computation, although the bearing capacity may be expressed in a limited general form in which the size of the footing and the cohesive shearing strength are variables. An important class of problems concerns itself with the examination of the failure conditions developed in a mass by the application of discontinuous normal stresses at the horizontal surface. The object of these studies is the computation of the ultimate load which can be carried by a footing at or near the surface of the ground, and the problem can be considered an extreme example of a sloping wall whose angle β to the vertical is equal to $-90°$. Sokolovski used techniques of numerical analysis to solve problems of this kind. He studied the superposition of the individual limiting conditions given by Terzaghi and concluded that the total stresses obtained at yield by summing the stresses at yield in the separate cases satisfy the appropriate equations of equilibrium. However, because of the nonlinearity he found that the yield condition for the superimposed stresses is that holding for a material whose angle of friction is smaller than the angle employed in obtaining the component stress states. Thus, for most materials, the superimposed solution will not correspond to the solution which would be found by means of a single exact analysis in which all material properties were included; the superposition solution yields a conservative result. Lundgren and Mortensen (16) made a theoretical study of a cohesionless material with an angle of internal friction of 30°, found that superposition gave a bearing capacity 17% lower than that of the

more nearly correct analysis.

Sokolovski found that if a dimensionless normal stress coefficient N_γ is employed to describe the slope of the line of increasing stress, the stress p_γ (here due to the unit weight of the material) can be obtained in the form:

$$p_\gamma = 2N_\gamma \gamma x \tag{1}$$

By a numerical integration of the two differential equations describing the yield conditions when the material has weight, Hajal found the correct curve of vertical stress distribution on the footing at failure. For different angles of internal friction of the material, Hajal found values of N_γ once again for a smooth or frictionless footing. Thus he obtained the limiting failure load per unit length of a smooth strip footing at a shallow depth z (where $z < 2b$) below the surface of a cohesionless material possessing weight.

$$\frac{p}{2b^2\gamma} = N_\gamma \left[2\left(\frac{h}{2b}\right) + 1\right] \tag{2}$$

Obviously a footing with a frictionless base represents an idealization which would rarely occur in practice, and then only in specially designed laboratory experiments.

The theoretical values of N_γ for a rough footing may be compared with the experimental results obtained by De Beer and Ladanyi (17) for a uniform sand, which indicate that N_γ has values of about 14, 33, 83, and 210 for ϕ of 25°, 30°, 35°, and 40°, respectively. For a somewhat coarser and less uniform sand, Feda (4) found that N_γ is about 170 for $\phi = 40°$,

and, on the basis of his own, other experiments, and a comparison with theoretical values, he proposes an empirical equation for N_γ:

$$N_\gamma = 0.01e^{0.25\varphi} \tag{3}$$

where e is the base of natural logarithms.

Bearing Capacity of Finite Blocks

Some work by German investigators was done on small blocks of concrete and rock. They performed some loading tests on strip and circular model footings resting on cubes of concrete and rock, Bauschinger (18), Graf (12), Bach and Baumann (11), in their work indicated that the materials fail by a combination of shearing and splitting. Immediately beneath the footing a wedge or cone of the material corresponding to an angle of internal friction of 40° to 50°, is formed by shearing along a rupture surface and is forced into the material below. By exceeding the tensile strength of the surrounding material, it is split progressively downwards and displaced sideways.

G. B. Sowers (19) performed some experiments on concrete specimens laterally supported in steel rings. He stated the looseness with which engineers use the term "compressive strength" when applied to brittle or comminutable materials such as concrete and rock leads to erroneous assumptions and even to unnecessary use of expensive and vital materials.

He showed that the true compressive strength of any area of rock or concrete fully supported laterally is several times greater than the compressive strength as developed by the simple cube or cylinder test.

Based on these and the observations of the German investigators Meyerhof (2) suggested a simple theory for the two dimensional case.

Meyerhof's Theory of Blocks

At the bearing capacity q_o of a strip footing of width B, resting on a block of thickness H and width L ($L \geq H$), the horizontal splitting pressure p_h can (in accordance with Coulomb-Mohr's theory) be shown to be

$$p_h = q_o \tan^2 \alpha - 2c \tan \alpha \tag{4}$$

whose resultant acts at a depth $\frac{B}{4} \cot \alpha$, where the semiwedge angle $\alpha = 45^\circ - \frac{\Phi}{2}$ (Figure 1). The maximum bending tensile stress p_t at the point of the wedge of material below the footing is

$$p_t = \left(1 + \frac{6H}{2H - B \cot \alpha}\right)\left(\frac{B \cot \alpha}{2H - B \cot \alpha}\right) p_h \tag{5}$$

simplifying

$$q_o = \frac{\left(\frac{2H}{B} - \cot \alpha\right)^2 \cot \alpha \; p_t}{\frac{8H}{B} - \cot \alpha} + 2c \cot \alpha \tag{6}$$

For large values of $\frac{H}{B}$ and substituting the unconfined prism strength $p_u = 2c \cot \alpha$.

$$\frac{q_o}{p_u} = 1 + \frac{H p_t}{4Bc}$$

This relationship indicates that the bearing capacity of surface footings is directly proportional to the ratio of block thickness to footings width $(\frac{H}{B})$ for a given ratio $\frac{p_t}{c}$ depending on the properties of the material. He also suggested that where splitting of the material is prevented by

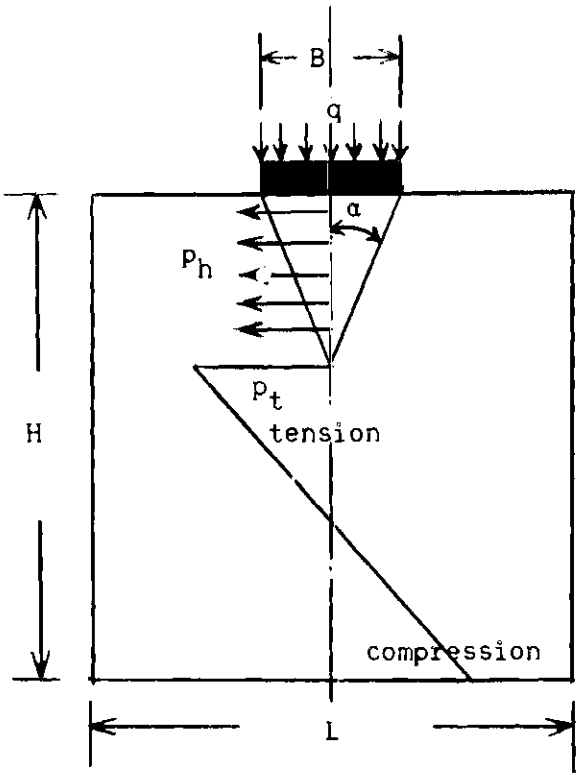

Failure of a Small Block

Figure 1. Analysis of Bearing Capacity of Rock Block, after Meyerhof.

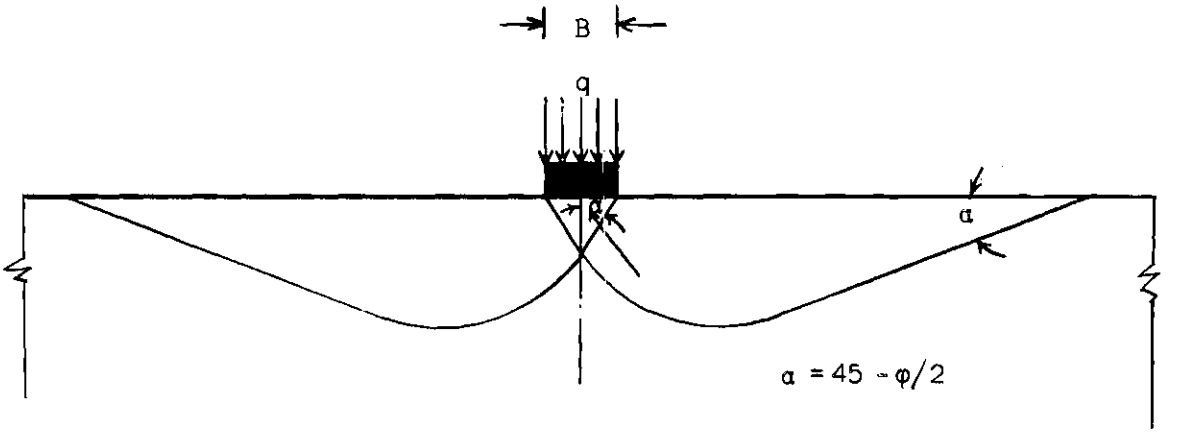

Failure of a Large Block

Figure 2. Analysis of Bearing Capacity of Rock Block, after Meyerhof.

reinforcement or the use of blocks that are large in relation to the size of the footing, the bearing capacity is mainly governed by the shearing strength of the material. At failure a wedge or cone is formed below the footing as before, but the material at the side is forced outwards and upwards by shearing along a curved rupture surface. The bearing capacity of a strip footing on the surface as before can then in accordance with Prandtl-Terzaghi approximately be represented by

$$q_o = cN_c \tag{7}$$

where N_c is the general bearing capacity factor. This factor depends mainly on the angle of internal friction φ and the ratio $\frac{L}{B}$ (or the inclination of the "equivalent free surface"). For a very large value of $\frac{L}{B}$ the bearing capacity becomes equal to that of a strip footing on the surface of a semi-infinite solid (Figure 2).

Meyerhof performed some model tests on concrete blocks using 1-1/4 inch circular footing. For splitting failure he suggested that the results can be analyzed in the same way as for the strip footings. For large blocks where the failure occur by general shear he extended the same theory used for strip footings to the circular ones on the surface. He suggested that bearing capacity is approximately given as:

$$q_o = cN_c + pN_q \tag{8}$$

where N_c and N_q are general bearing capacity factors for circular footings and p is the normal pressure on equivalent free surface. For a large value of $\frac{L}{B}$ the bearing capacity becomes equal to that of a circular footing on the surface of a semi-infinite solid.

Meyerhof's theory in cases of splitting failure suggests the same bearing capacity for blocks with $L \geq H$. This contradicts the experimental results of Von Kolnitz (20) and Johnson (21), where it is seen that the bearing capacity increases with the width of the block.

Meyerhof also suggested the failure by general shear takes place at large ratios of footing width to block width and thickness. But he did not give any ratios of footing size to block size at which such a failure will be expected.

Von Kolnitz

Von Kolnitz (20) investigated the bearing capacity for rectangular footings of a thin layered, jointed rock system. He used square footings of 1", 2", 3", 4", and 6" size, with 4" x 4" x 1" thick blocks. On the basis of his experimental data he suggested a modification of the Meyerhof's equation for his jointed rock system. Von Kolnitz summarized the results of his investigations as follows:

1. There was no significant transfer of stress across the discontinuities. The only blocks affected were those directly beneath the footing.

2. Based on the above statement and results, no attempt should be made to analyze the bearing capacity of a jointed rock system with the general bearing capacity equation, unless the foundation is very small in comparison to the block.

3. The bearing capacity of the jointed system can be evaluated by a simple modification to the Meyerhof's equation for the bearing capacity of rock:

$$q_o = \left\{ \frac{\left(\frac{2H}{B} - \cot\alpha\right)^2 (\cot\alpha)\, p_t}{\frac{8H}{B} - \cot\alpha} + 2c\ (\cot\alpha) \right\} \frac{H}{B} \qquad (9)$$

4a. Small footings: When the footing is small compared to the block size, there is a slight increase in bearing capacity when the footing is moved from the center to the edge of a block. Further, there is a significant drop in bearing capacity when the footing is moved to the corner of a block and over a discontinuity.

4b. Large footings: When the footing size approaches the block size, position of the footing affects the bearing capacity very little until a discontinuity is covered. This results in a significant drop in bearing capacity.

5. Failure occurs in a splitting manner followed by a punching out of lower blocks.

6. Settlement depends greatly upon the tightness of the packing of individual blocks and would be most difficult to predict.

According to Von Kolnitz the modification to the Meyerhof equation does not hold when the footing size is increased so that it exceeds the block width, as in the case of the six-inch footing. When this was done, the bearing capacity remained very nearly that for the four-inch footing. This suggests that the bearing capacity reaches a lower limit when the footing width is just equal to the block width. Another feature here was that the constant value for bearing capacity was reached when the footing was centered over a vertical discontinuity. This also held true when the smaller footings were centered over two blocks and then over four blocks. His statement that bearing capacity increases when the footing is moved

from the center to the edge of block does not seem to be correct, as the work done by Johnson (21) also at Georgia Tech shows that the bearing capacity decreases in that case.

Von Kolnitz pointed out that this modification holds true only when the footing width exceeds the rock thickness. If the reverse were true, the modification would result in an increase in bearing capacity. It should also be pointed out that this modification may not hold if the rock layers become very thin as in the case of laminated rock. If the thickness of the layer should approach zero, the predicted bearing capacity would also approach zero, which does not seem reasonable.

Johnson

Johnson (21) further worked on the jointed rock system. He used a thin layered, jointed system composed of small blocks (four inches square by 0.25 inch thick) of Indiana Limestone stacked as closely as possible by hand to form a mass 12 inches square and four inches high. The system was placed on a rigid aluminum retaining box, two adjacent sides of which were fitted with SR 4 strain gauges for measuring the lateral loads which developed during testing. Model footings were made of steel and ranged from 1.25 inches square to six inches square. The rate of deformation was 0.01 inches per minute.

He found a general trend for bearing capacity as a hyperbolic function of the ratio of footing width, B, to block width, L. The amount of settlement occurring in the loaded blocks was found to be dependent upon the thickness of the separations occurring in a horizontal plane between the stacked blocks. Lateral loads appeared to reach "critical magnitudes" with regard to foundation failure only after the loaded blocks had failed

in bearing. He gave the following conclusions:

1. The bearing capacity failure occurring in the loaded blocks is always the splitting type described by Meyerhof.

2. The bearing capacity of the loaded blocks can be represented by a power function of the form

$$q_o = a\left(\frac{B}{L}\right)^n \tag{10}$$

in which a is in psi units and n is a fractional negative exponent.

3. The magnitude of the coefficient a and exponent n vary according to the position of the footing on the loaded blocks.

4. The total amount of settlement occurring in such a system prior to failure can be attributed to the following: an initial component due to the reduction of void spaces occurring in a horizontal plane between stacked blocks, and a subsequent quasi-elastic component resulting from deformation of the individual blocks under load.

5. In order to predict the amount of settlement which would result in the loaded blocks, it would be necessary to determine the thickness of void spaces present in the system prior to loading, and to determine the behavior of the quasi-elastic deformation of the system.

6. The lateral load developing in such a system under a footing load is probably dependent upon the Poisson's ratio of the rock, the irregularities in individual blocks and stacking, and the width of void spaces occurring in a vertical plane within the system prior to loading.

7. The lateral load developing in such a system prior to failure is not of sufficient magnitude to be a factor in foundation failure.

8. Lateral load developing after failure of the loaded blocks is due to the forcing aside of adjacent blocks by the wedge of material formed underneath the footing as it is forced downward.

The results of Von Kolnitz and Johnson clearly showed that the bearing capacity varies with $\frac{B}{L}$ ratio, i.e., the ratio of the block width to the footing width. This indicates clearly the limitations of Meyerhof's analysis. But as each of the above investigators performed tests on just one thickness of the blocks, the investigations only serve the purpose of indicating that the bearing capacity varies with the width of the blocks also. The curves of q_o vs. $\frac{B}{L}$ given by Johnson clearly states the above fact.

CHAPTER III

INSTRUMENTATION AND EQUIPMENT

The rock selected for testing in this investigation was Indiana Limestone. The rock can be cut freely, without splitting, into the desired shape and dimensions. As a large quantity of material was necessary to be cut into shapes and different sizes, this particular rock was chosen for the investigation.

Indiana Limestone is found in an area around Salem, Indiana. The rock is composed of limestone "sand" grains cemented together by the interlocking action of calcite crystals. The "sand" grains are the result of deposition of calcium carbonate on small, partially broken shells, often in a series of concentric layers. Due to their roughly spherical shape resembling fish eggs, the rock is termed by geologists as "oolitic" limestone. It is a calcite cemented calcareous stone formed of shells and shell fragments, practically non-crystalline in character. It is characteristically a free stone without pronounced cleavage plane, possessing a remarkable uniformity of composition, texture, and structure and equality of strength in all directions regardless of the plane of its natural bedding (23). The average analysis (in per cent) as developed by carefully prepared composite samples of Indiana Limestone Company shows that it contains 97.39 per cent Carbonate of Lime, 1.20 per cent Carbonate of Magnesia, .69 per cent Silica, .44 percent Alumina, .18 per cent Iron Oxide, .10 per cent Water and Loss.

The average weight of dry (seasoned) Indiana Limestone is 144 pounds per cubic foot.

The stone varies in colortone from buff to grayish or blue-gray shade. Dark spots are sprinkled throughout the rock, which seems to be the organic residue of the original inhabitants of the shells. The unconfined compressive strength of the rock varies from about 4000 to 12,000 psi (22, 23).

Types of Tests

The types of tests performed in this investigation covers,

1. Triaxial Cell Tests
2. Bearing Capacity Tests
   a. Open Jointed System
   b. Closed Jointed System
3. Plane Strain Tests

Triaxial Cell Tests

The special Triaxial Cell, designed and built at Georgia Institute of Technology to test rock samples under lateral pressures of up to 10,000 psi was used for these tests. The pressure cell is constructed of bearing bronze, high strength steel, and stainless steel. The base contains the ports for the lateral confining pressure and pore pressure.

A high strength steel pedestal was fitted at the center of the cell base to act as a base for the rock samples to be tested. A high strength steel cylinder was threaded on the base and an O-ring was provided for the sealing purpose. A bronze packing gland threaded into the top of the cylinder formed the upper seal. In the center of the packing gland a stainless steel piston, sealed with four o-rings was provided for

the loading. The piston was brought in contact with the upper end of the rock sample, while testing, and was thus used for applying the vertical loading. Two small loading blocks of stainless steel, 7/8 inch in diameter, were used on each side of the rock sample. The small loading blocks were flat on one side and spherical on the opposite sides. This was done to match the spherical depressions in the base and the piston with the side of the loading blocks and the flat side to match the sides of the rock sample. This arrangement was helpful to take care of slight misallignments incurred during sample preparation. In order that the air can escape as the cell was being filled with hydraulic oil, a value was provided at the top of the cylinder. The confining pressure was controlled by using high pressure hand pump. The hand pump was connected to the base through which the oil was pumped into the cell. The confining pressure could be increased by pumping the oil in the cell by the hand pump or could be released by means of a screw value provided for the same.

Preparation of the rock samples was accomplished by using conventional machine tools which had been modified for the use of rock cutting and rock coring apparatus. A twelve-inch diamond tooth circular saw was used to trim the rock specimens to suitable size and shape for coring. Two parallel faces were cut, producing a slab approximately two inches thick. In the sedimentary rocks these faces were cut parallel to the stratification so that the test core would be oriented in its natural position when placed in the triaxial test cell. A diamond impregnated coring bit, 7/8 inch inside diameter and one inch outside diameter, was used to produce a core sample from the previously prepared slabs. The coring bit was attached to a water head and was driven by a conventional

drill press.

A suitable material for use as a membrane must be impervious with respect to the confining fluid and must be sufficiently flexible so that the sample deformation is not restricted. A material meeting these specifications is plasticized polyvinyl chloride plastic in the form of thin wall tubing. The tubing used was 7/8 inch inside diameter with a 0.035 inch wall thickness.

Axial deformations were measured during testing by using a micrometer dial indicator having divisions of 0.0001 inches. The dial indicator was placed between the load table and the crosshead of the testing machine. Also the axial deformations were simultaneously measured by using a linear variable differential transducer. The load-deformation curve was traced on a drum recorder, with the axial load indication being actuated by a push-rod arrangement from the testing machine load indication unit.

The loading machine used in the triaxial shear tests for loads up to 20,000 pounds was a controlled strain mechanically driven machine, with deformation rates of 0.01 inches per minute. The test set up using the machine is shown in Figure 5.

Bearing Capacity Tests

Tests on two types of jointed systems were performed.

a. Open Jointed Rock System

b. Closed Jointed Rock System

An open jointed system will be referred to here as "a jointed rock system in which the blocks adjoining the loaded blocks will have negligible or no effect on the bearing capacity of the loaded blocks" whereas, "in a closed jointed system the adjoining blocks will have a significant

effect on the bearing capacity of the loaded blocks."

The loading tests were done on three types of footings in each case.

The shapes of the footings used were:

1. Circular Footings

2. Square Footings

3. Strip Footings

The diameter of the circular footings used were, 1", 2", 3", and 4". The square footings were squares of 1", 2", 3", and 4" sides. The strip footings were 5" long and had widths of 0.35" and 1/2" respectively.

The rock used in the testing was cut into the desired shapes of the blocks. Different combinations of lengths, widths and thickness of the blocks were used for different tests. In case of open jointed system, the thickness of the blocks varied from one inch to sixteen inches and the width from two to sixteen inches. It was desired to test greater size blocks with width and thickness of about twenty four inches but the sizes had to be restricted because of the limited availability of the material. The details of all the sizes used for the bearing capacity tests are given in chapter headed Test Procedure.

Two multiple range driven, controlled strain testing machines, one mechanical and one hydraulic, were employed in conducting the model footing tests on the jointed rock system. These were the Tinius-Olsen Machines, the one used in conducting the unconfined compression tests on the cylindrical samples having a capacity of 20,000 pounds and the other having a capacity of 120,000 pounds. Deformations of the loaded blocks were measured with a micrometer dial gauge sensitive to 0.0001 inch. Also the

deformations were simultaneously measured by using the linear variable differential transducer and the load deformation curve was traced on the drum recorder as in the case of triaxial tests.

A rigid aluminum box enclosed on four sides and the bottom was used to retain the system. The sides of the box were made from six inches x 0.25 inch aluminum flat stock, and were fitted with two pieces of one inch x 0.25 inch aluminum angle which acted as stiffeners. The bottom of the box was 13.625 inches square and 0.25 inch thick. It was attached to two adjacent sides of the box with one 0.125 inch brass screw per side. The size of the box had to be limited, keeping in mind the amount of material required for a single test, and the time needed for cutting the proper size and number of blocks required to fill the box. When testing 2" x 2" blocks, 144 blocks were needed to fill the box for each test.

The sides of the box were mounted with SR4 Strain Gauges, to determine the lateral stresses transferred to the sides of the box, during testing. The same system was used during the tests on closed jointed system. In the closed jointed system, the blocks were given a confinement pressure by the sides of the box prior to the testing. With this system, which is shown in Figure 3, it was possible to give an initial confinement pressure to the jointed rock system. This was achieved by the help of the strain indicator box, by inserting thin rock shims between the sides of the retaining box and the rock system. Also as an additional check, a thin disc shaped load cell was placed between the rock system and the side of the box. With the help of the strain indicator box, it was possible to find the load transferred to the side of the box. The load cell and the sides of the box which were loaded as simple beam, were calibrated

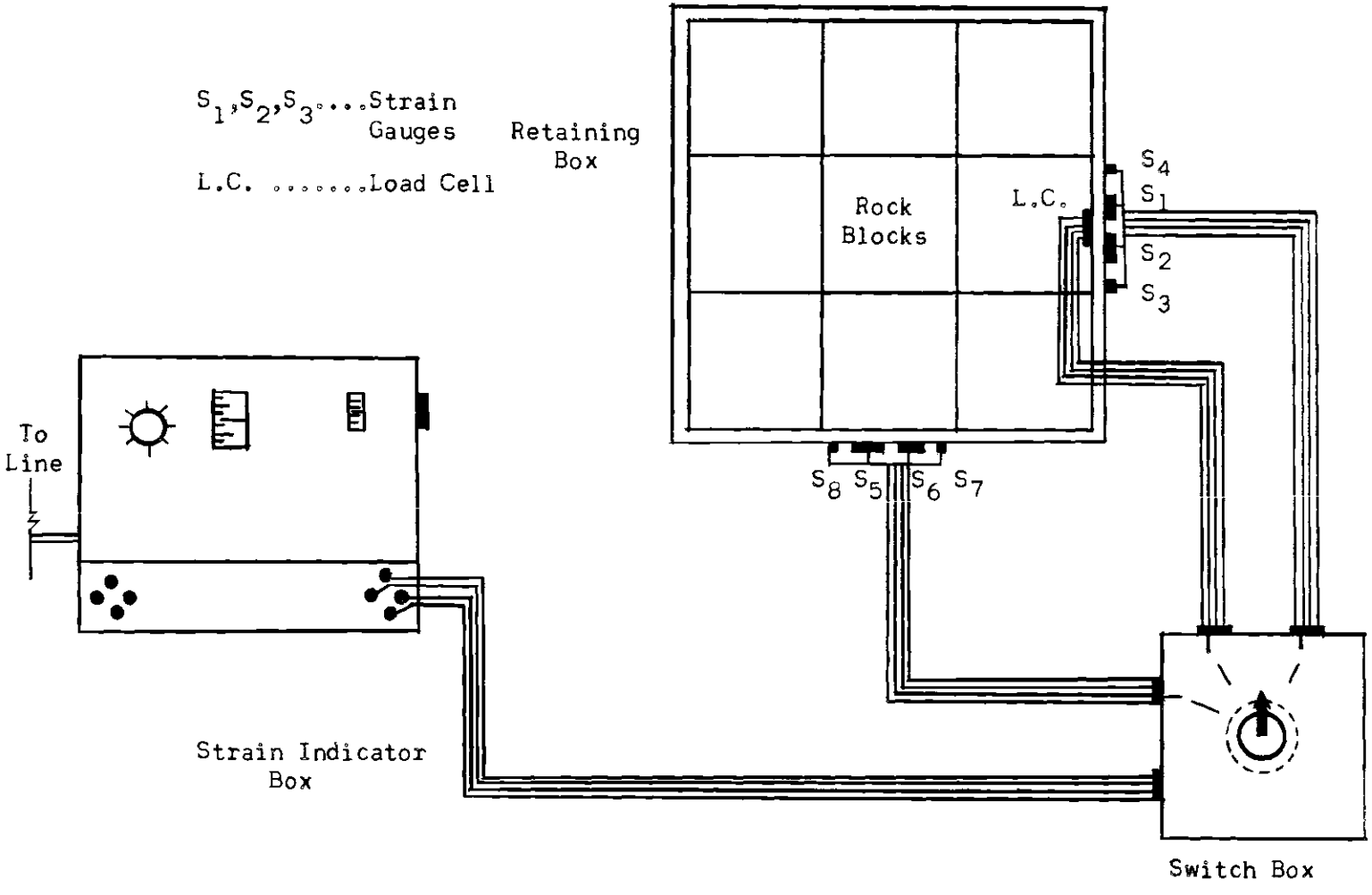

Figure 3. Strain Gauge Arrangement for the Testing of Jointed Rock System.

for the response of the load before testing. A simple switch box and a strain gauge indicator box were used to take different responses of the sides and the load cell during the testing. A schematic diagram of the system is shown in Figure 3.

Some tests were performed on a single column of blocks in the big triaxial cell of one foot diameter used in the plane strain tests. This was done as a check on the bearing capacity tests done in the box. Air pressure was used from the compressor for the confining pressure. For performing these load tests of 1", 2" and 3" circular footings over 4" x 4" x 1" blocks, a column of four blocks was used to simulate the central column in the jointed rock system in the box. The cell was modified for this purpose. Two aluminum blocks were designed and made to fit the cell as shown in Figure 4.

The curvature of the blocks was made to fit the cell curvature. The upper blocks had a groove for the cell piston to slide through and apply the load to the footing which was placed below it. The lower block was built with a sliding wedge arrangement for the minor adjustment with regard to the small variations in the height of the blocks. The upper block was fixed to the cell by means of four bolts which were screwed into the body of the cell. Air was used from the air compressor for the confinement and was read by means of a gauge attached to the body of the cell. Rubber membranes were used for testing in this case.

Plane Strain Tests

Some plane strain tests were conducted on the rock samples in this investigation. The length of the rock samples used was 16", the width 2",

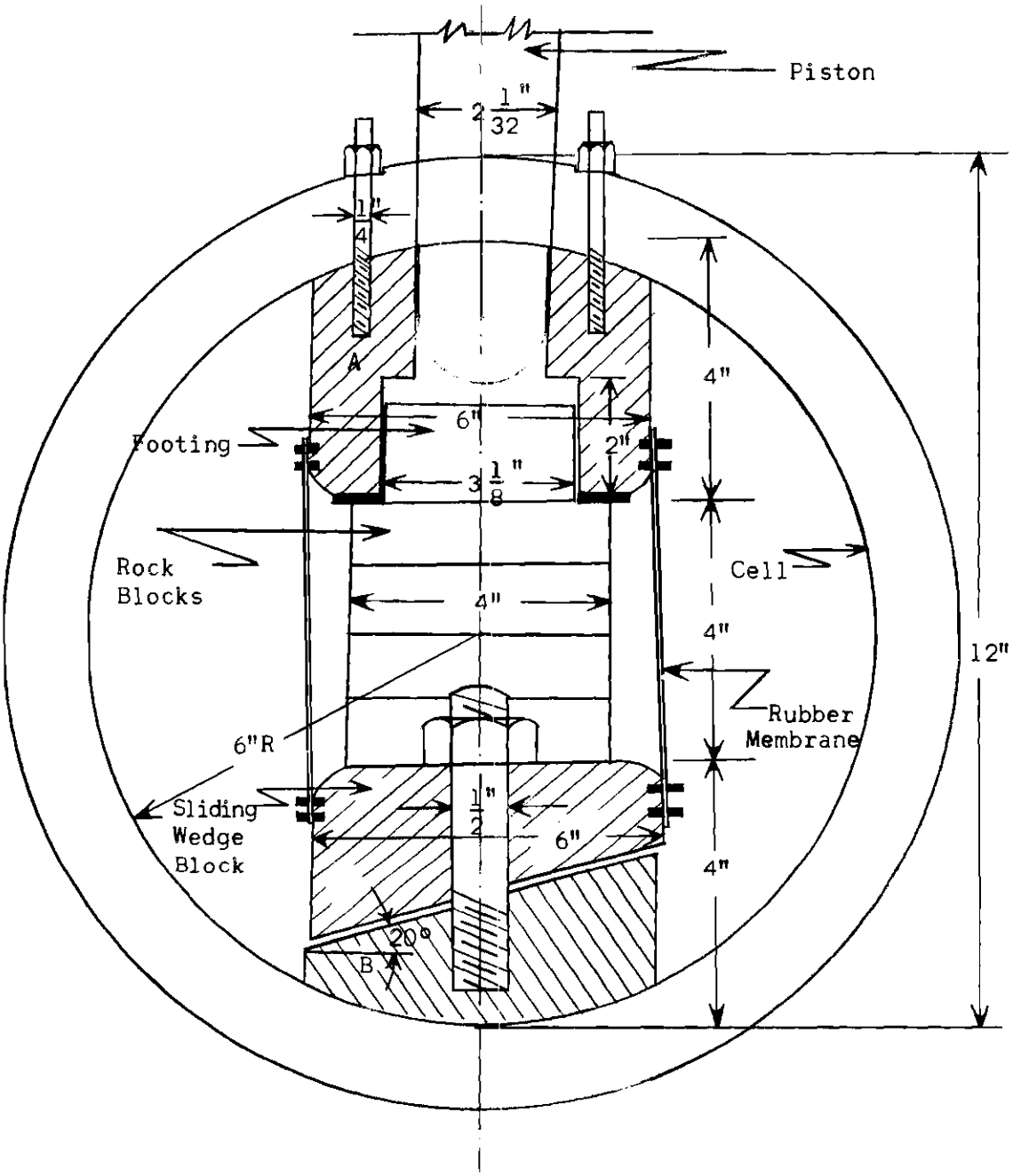

Figure 4. Cell Cross-Section Showing Arrangement for the Bearing Capacity Tests Inside the Cell.

and height 4". The rock samples were cut for this purpose from bigger blocks of rock with a diamond saw.

The plane strain apparatus designed and built at Georgia Institute of Technology was used for the testing. The cell was formerly used with air pressures of only up to 300 psi. It was planned to test the rock samples up to a pressure of 1000 psi, so it was necessary to use fluid for confinement at this higher pressure, rather than air. For this purpose it was decided that oil would be more suitable to use than water, because of the complicated wiring system in the cell. An ordinary lubricating oil No. 10 SAE from Sinclair Petroleum Products obtained from Sinclair Refining Company was used for this purpose.

A new load cell was designed and built in the laboratory for the purpose to record the intermediate principal stress and which could be used in oil. The body of the load cell was made in the laboratory using high strength steel. The load cell was designed to take loads up to 5000 pounds. SR4 strain gauges were mounted on the body of the cell in order to measure the stress response of the cell. The load cell was then calibrated with the help of the loading machine and strain indicator box. New sensors for keeping the length of the sample constant were made to suit the new conditions and also the entire electrical circuit had to be insulated, so as not to get short circuited when in touch with oil. For this purpose Duco epoxy cement was employed at certain places.

The oil was accumulated in a large tank from which it was pumped by means of a motor into the cell and back. Gauges were fixed to the cell to record the cell pressure. For controlling the cell pressure and the intermediate principal stress, in order to keep the length constant, high

pressure hand pumps with valved lines connected to the fluid inlet ports on the cell were used.

As with the previous experiments on the plane strain apparatus, it was found necessary to produce rubber membranes in the laboratory from the latex solution than to obtain commercially made ones. The membrane mould was dipped into the latex bath approximately seven to eight times. For dipping the mould into the latex, it was slowly immersed into the bath so as not to create air bubbles allowing about a minute to elapse, and then slowly withdrawing it until the top was just above the surface of the latex. Further time was permitted for the excess solution to run off the top of the mould before it was removed from the bath. The process took about three minutes, after which the mould was hung up to dry for a minimum of two hours. To obtain an even membrane thickness, the mould was inverted for alternate dippings, and extra latex was applied to the corners between dippings.

When the final dipping was completed, the membrane was allowed to cure on the mould for 24 hours. The upper and lower surfaces were cut away to fit the platens of the plane strain apparatus, and the membrane was carefully stripped from the mould. After being checked for holes or imperfections, the membrane was put away to cure for another two days before use.

The intermediate principal stress was applied by means of a hydraulic jack connected to a high pressure hand pump. The readings of the applied load were recorded by the load cell placed at the other end of the sample. Sensors with the help of strain indicator box were used for the purpose of keeping the length of the sample constant. Details of the procedure used are given in Chapter IV.

CHAPTER IV

TEST PROCEDURE

Triaxial Cell Tests

Preparation of the samples for the triaxial tests was accomplished by using a diamond impregnated coring bit, 7/8 inch inside diameter and one inch outside diameter. The coring bit was attached to a water head and was driven by a conventional drill press. The samples were then cut to the 2" size and their ends polished smooth. The samples were then left for a few days for air drying before use.

The core sample along with the loading blocks and membrane, was placed on the cell pedestal, the rubber o-rings were slipped over the ends of the membrane. The membrane was kept longer than the sample, so that it would also cover the small loading blocks placed on both sides of the sample and then slip over the steel pedestal on the base of the triaxial cell. The overlapping ends of the membrane were sealed by using 4 o-rings over the jacket at each end. The cylinder was assembled to the base and filled with hydraulic fluid to the level of the vent valve opening. The packing gland was then secured in position, but remained at least 1/4 turn from a fully tightened condition.

To test the membrane and its seals for leakage an oven dry limestone sample was placed in the triaxial cell and the lateral pressure increased to 2,000 psi. When the pressure was released and the sample removed, it was examined for any spots of oil which would readily be

visible on the light colored surface. No leakage was detected in this case. After assembly the triaxial cell was placed in the testing machine and the lateral confining pressure hose connected to it from the high pressure hand pump, and the confining pressure applied.

The deformation rate used was 0.01 inches per minute in all the tests. The deformation readings were taken at regular intervals of loading. The loading increments were chosen as 100 lbs. in some tests and 200 lbs. in others. The consecutive deformation readings become larger as the samples approached failure. As the failure was reached the load decreased rapidly in most of the cases. A higher rate of deformation of 0.02 inches per minute was applied to the samples after failure.

Bearing Capacity Tests

Various sizes of blocks were used for each type of test to get a comprehensive picture of the effects of different dimensions on the bearing capacity. However, in the closed jointed system, the experiments were performed on 4" x 4" x 1" and 2" x 2" x 1" blocks and some strip blocks only. The limitations had to be put, keeping in mind the difficulties involved in preparing a closed jointed system and the quality of the materials involved.

The sizes of the rock blocks used for open jointed system were varied in width dimensions from 2" to 16" and the thickness of the blocks varied from 1" to 16".

The various sizes used for circular and square footings are as follows:

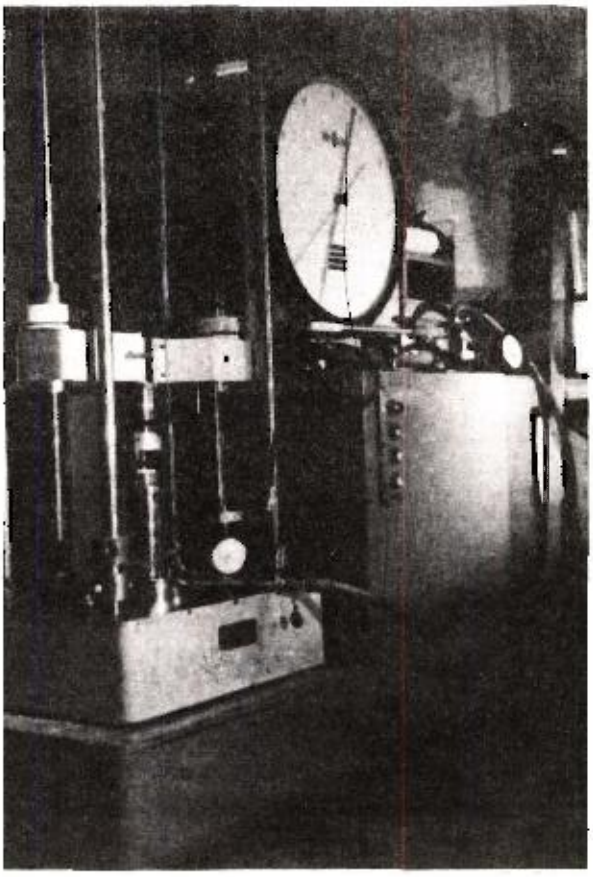

Figure 5. Triaxial Test Set Up.

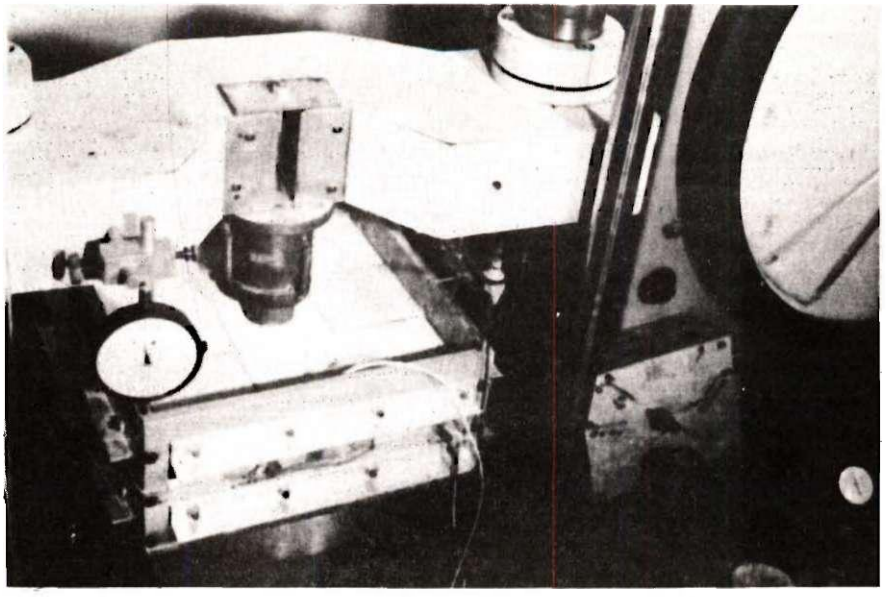

Figure 6. Bearing Capacity Test Set Up for Jointed Rock System.

Length	Breadth	Thickness
2"	2"	1"
2"	2"	4"
4"	4"	1"
4"	4"	4"
4"	4"	8"
4"	4"	10"
4"	4"	16"
8"	8"	4"
16"	16"	4"

The sizes of blocks used for strip footings are as follows:

Length	Breadth	Thickness
5"	1.40"	4"
5"	2"	4"
5"	3.5"	4"
5"	4"	4"
7"	5"	4"
8"	5"	4"
14"	5"	4"
16"	5"	4"

For the open jointed system, the samples used in the model footing tests were sawed with the masonary saw as previously described. After sawing, the blocks were air dried for a few days. In order to provide as smooth a bearing surface as possible and to avoid any flexural deformation

of the blocks, both faces of the sample were ground and made level. The final tolerances in the block thickness and width were ±0.015 inches.

The blocks were then arranged in the aluminum retaining box. The box was previously assembled on the bed of the testing machine, and the SR4 strain gauge was inspected to insure that it was functioning properly and the zero readings taken. The individual blocks were then stacked on as closely as possible by hand in the retaining box as shown in Figure 6. Thin rock shims were placed between the system and the two adjacent sides of the box to insure transmission of any lateral load which developed during testing. In this case care was taken that no initial confinement was produced on the system, while keeping these shims in position, which could be easily checked by means of the SR4 strain gauge system. As an additional check, the disc shaped load cell was placed between the system and the side of the box, and any load transferred to the load cell could thus be recorded by means of the strain indicator box. The model footings were then placed in the appropriate position in the center of the central block. The loading head was then brought into contact of the footing and a seating load of approximately 10 pounds was placed on the footing. The micrometer dial gauge used to measure deformation in the loaded blocks was placed in position and adjusted to zero reading. The zero readings of the strain gauges and the load cell were recorded. Also the linear variable differential transducer was adjusted for zero reading and the recording drum was brought in position and the marker ink pen was placed on the graph paper mounted on the drum for the load settlement curve.

The footing load was applied at a rate of deformation of 0.01 inch per minute. The system was loaded until the footing load reached a maximum

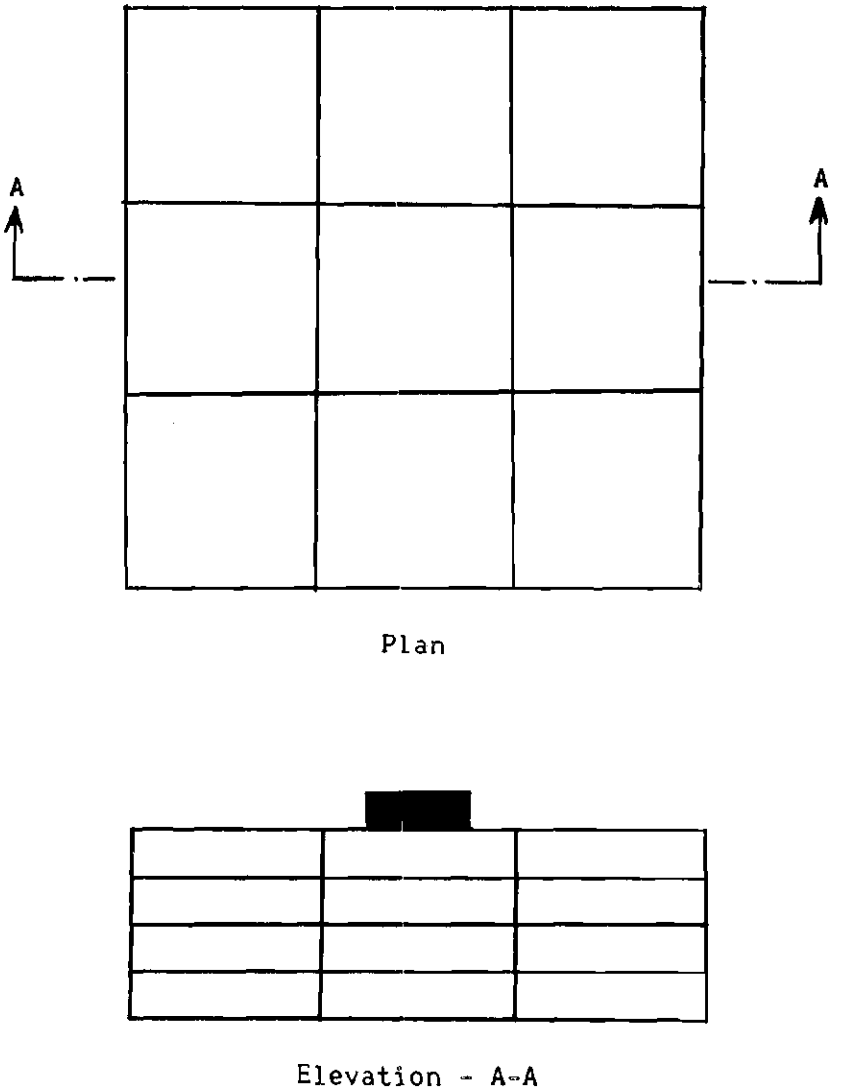

Figure 7. Block Arrangement for the Bearing Capacity Tests on Jointed Rock System.

value and failure occurred, and continued in some cases after failure. The strain gauge readings and also the load cell readings were taken from time to time during testing.

For the closed jointed system the same procedure was used as indicated for the open jointed one. In case of open jointed system it was taken care that the system was not confined by the sides of the box at the start of the test. But in the closed jointed system, an initial confinement pressure of the desired value was applied by the sides of the box, using the SR4 strain gauge device and the load cell. The initial confinement pressures used in this investigation were 20 to 100 psi. The confinement pressures were achieved by pressing thin rock shims between the sides of the box and the rock system and varying the thickness of the shims and watching the stress produced at the side of the box. By maintaining the desired value of indicated strain it was possible to keep the desired confinement pressure on the rock system. An additional check was done every time as before by the use of the disc shaped load cell which was kept between the rock system and the side of the retaining box.

The closed jointed rock system tests were done on blocks having thicknesses of 1" and 4". The width dimensions used were 2" and 4". Various sizes used for circular and rectangular footings are as follows:

Length	Breadth	Thickness
2"	2"	1"
4"	4"	1"

For strip loading tests the sizes of the blocks used are as follows:

Length	Breadth	Thickness
5"	3.5"	4"
5"	4"	4"

In order to achieve a greater accuracy, two different machines were used, depending upon the magnitude of the desired load. The bearing capacity test set up is shown in Figure 6.

Some bearing capacity tests were done on 4" x 4" x 1" blocks, using circular footings of 1", 2" and 3" diameter, in the big cell of 1 foot diameter. This was done to see the difference in bearing capacity of the system with the confinement produced by the adjacent blocks on the central column of blocks as in the jointed rock system, and in a system where the confinement on the central blocks was due to the air pressure in the cell. The details of the arrangement for this test are shown in Figure 4.

The rock blocks were placed on the pedestal over the lower block in the cell, having the sliding wedge arrangement. For convenience, the rubber membrane was first slipped over the lower block before the rock blocks were put on it and o-rings put around the membrane, to seal the blocks from the outside pressure in the cell. After keeping two blocks it is easy to keep the upper block with the footing in the center held in contact with the upper aluminum block and then to slide the middle block between them. After the blocks were placed in position the sliding wedge block was pushed up a little, by sliding the upper wedge in the block, over the lower wedge thus butting the rock blocks with some pressure against the upper aluminum block. Then the membrane was slipped over the upper block and o-rings put around it.

The piston was then brought in contact with the footing. The cell

was filled with air from the air compressor and the desired confinement pressure applied, which could be read by the gauge attached to the cell. An initial load of about 20 pounds applied and the deformation dial gauge was set for zero. The deformation was read by means of a dial gauge divided into divisions of 0.0001". The load was applied by means of the loading machine attached with the plane strain apparatus. The rate of deformation was kept at .01 inch per minute.

Plane Strain Tests

Plane strain tests were run on rock samples of size 2" x 4" x 16". The sample dimensions were checked before use. The rubber membrane was fixed to the bottom platen by keeping the membrane between the bottom plate and the platen and tightening the two by means of the screws. Then the rock sample was put in the membrane and the upper platen was placed over it. The membrane was carefully kept between the upper platen and the loading cap and the two were tightened against each other by means of the screws provided for the same. The load cell was then placed on one end of the sample and was connected to the other side of the sample with a hydraulic jack by means of high tension steel bars. The hydraulic jack was provided to give the intermediate principal stress.

The sensors were then put together, one on each side of the sample, along its length and were joined to two end plates put on the ends of the sample. Then the hydraulic jack was connected to the high pressure hand pump which was used for giving the pressure to the jack, and a check was made on the sensors which were connected to the strain indicator box. The two end plates on the sample were brought in contact at the ends of the

sample by tightening the screws of the high tensile steel bars by hand and a little pressure applied.

The whole assembly was then slowly lifted and taken inside the cell, and placed in position. The cell assembly was lifted by means of the motor, until the loading piston was in place and in contact with the loading cap, placed over the sample. The piston and loading cap were connected by means of an Allen Key, put across two holes in the angles screwed on the loading cap and through the hole in the piston. This was done to insure that the piston was in place over the center of the sample throughout the test. An initial load of about 100 pounds was then applied to the sample, and the micrometer dial gauge was adjusted to zero position.

Before starting the test, the zero reading of the load cell for the intermediate principal stress was taken with the strain indicator box. The reading for the sensors was taken and was kept at this reading throughout the test, by means of the hydraulic jack. The cell was then closed by placing the side cap in position by means of the screws.

The cell was then filled with oil by means of the motor. The confinement pressure was applied by means of the other high pressure hand pump used for this purpose. The zero readings were again taken, before the start of the loading. The loading was done at a deformation rate of 0.01 inch per minute, and for loading, the machine attached to the plane strain apparatus was used. The intermediate stress was increased during the test to keep the length of the sample constant and recorded with the help of the load cell and the strain indicator box. Throughout the test, the longitudinal sensor reading at the strain indicator box was kept the same, thus insuring the length to be constant throughout the test.

CHAPTER V

THEORETICAL DEVELOPMENT

Theoretical expressions have been developed in this chapter for the bearing capacity of circular footings resting on square blocks forming the jointed system. The expressions are developed, both for blocks with very low and high $\frac{H}{B}$ ratios. Earlier work done on similar materials show that the Mohr-Coulomb failure criteria can be used for the yield condition (23).

The following failure mechanism is postulated for calculating the bearing capacity of a circular footing resting on a square block of the jointed rock system.

When the footing load is increased, a cylindrical zone of material below the footing develops a state of stress corresponding to plastic equilibrium. The horizontal or radial pressure of this cylinder creates an internal pressure on an external cylinder of rock surrounding it. Further increase in the load on the footing increases the horizontal splitting pressure correspondingly. With the increase in the horizontal splitting pressure the external cylinder of rock which surrounds the material below the footing also starts to become plastic. When a sufficient part of this surrounding material has become plastic, the failure of the external cylinder takes place, by splitting.

The horizontal splitting pressure, p_h, at failure is assumed to be the inside pressure of the expanding cylinder, whose inside diameter is the diameter of the circular footing and the outside diameter as the

diameter of the loaded cylindrical blocks. For rectangular blocks, which have been used in this investigation, the outside diameter is assumed conservatively to be the diameter of the inscribed circle. The horizontal splitting pressure, p_h, is then related to the bearing capacity, q_o, by the Mohr-Coulomb failure criteria.

For blocks of higher $\frac{H}{B}$ ratios the horizontal splitting pressure, p_h, is taken as the inside pressure of an expanding long cylinder, which due to axial symmetry, assumed here, will be in plane-strain condition. For very thin blocks, with low $\frac{H}{B}$ ratios, the inside expanding pressure required for failure is calculated, treating it as a very short cylinder or in other words a flat ring. This is a case of plane-stress as the longitudinal stress becomes zero for all points. Due to the axial restraint in a long cylinder the expanding pressure will be higher and, consequently, the bearing capacity will be higher for blocks of greater $\frac{H}{B}$ ratios in comparison to the thin blocks forming a short cylinder.

At the outside diameter a pressure p_o is considered to act for the case of a closed jointed system and which is taken as zero for the open jointed rock system.

The following assumptions are made to calculate the theoretical bearing capacity of a circular footing resting on square blocks forming a jointed system.

1. The material is taken as homogeneous and isotropic in character

2. Ideally plastic material.

3. Failure takes place when yielding occurs over the plastic region and all the material has become fully plastic.

4. The yield condition is defined by Coulomb's equation. Taking

σ_r and σ_θ as major and minor principal stresses,

$$\sigma_r = \sigma_\theta N_\varphi + 2cN_\varphi^{1/2} \tag{11}$$

where $N_\varphi = \tan^2 (45 + \varphi/2)$

(a) For high $\frac{H}{B}$ ratios.

For an element in cylindrical coordinates assuming radial symmetry and no variation in the axial direction, considering the equilibrium of a volume element bounded by two concentric cylindrical surfaces the equation of equilibrium for a cylinder are reduced to (Figure 8)

$$(\sigma_r + \frac{d\sigma_r}{dr} \cdot dr)(r + dr)\, d\theta \cdot dz - \sigma_r r\, d\theta\, dz - \sigma_\theta \cdot dr \cdot d\theta \cdot dz = 0$$

or

$$\frac{d\sigma_r}{dr} + \frac{\sigma_r - \sigma_\theta}{r} = 0 \tag{12}$$

where σ_r and σ_θ are the radial and tangential stresses (27). Solving the differential equation, with the help of equation (11) gives

$$\sigma_r = \frac{1}{(\frac{1}{N_\varphi} - 1)} \left[Ar^{(1/N_\varphi - 1)} + \frac{2c}{N_\varphi^{1/2}} \right] \tag{13}$$

and

$$\sigma_\theta = \frac{1}{(\frac{1}{N_\varphi} - 1)} \left[\frac{Ar^{(1/N_\varphi - 1)}}{N_\varphi} \right] + \frac{2c}{N_\varphi^{1/2}} \left[\frac{1}{N_\varphi (\frac{1}{N_\varphi} - 1)} - 1 \right] \tag{14}$$

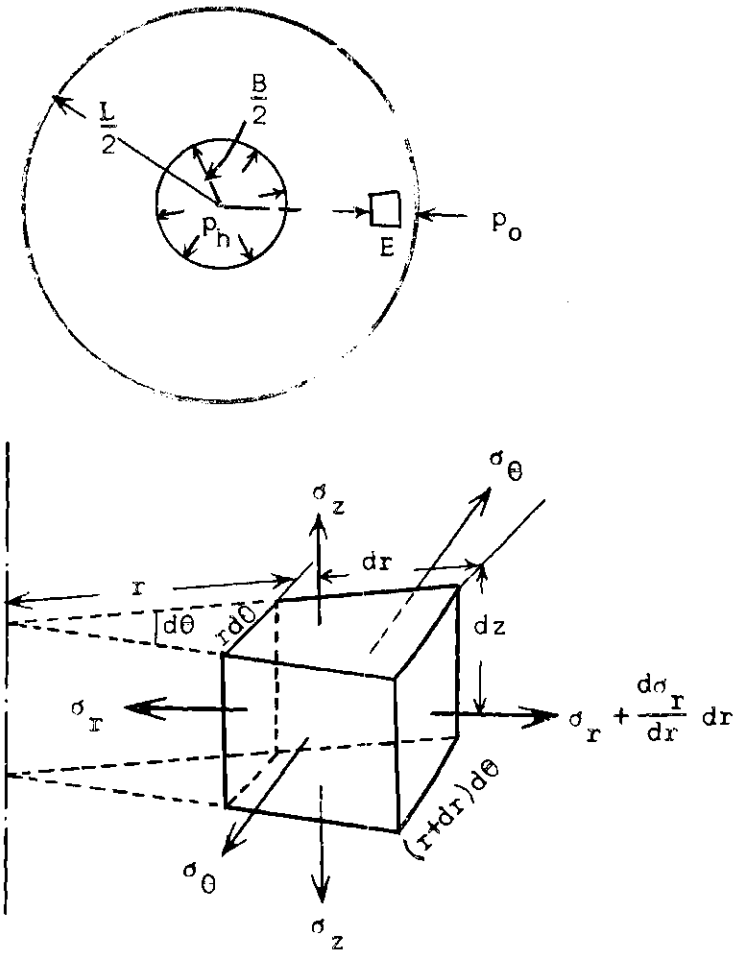

(a) Stresses on Volume Element E

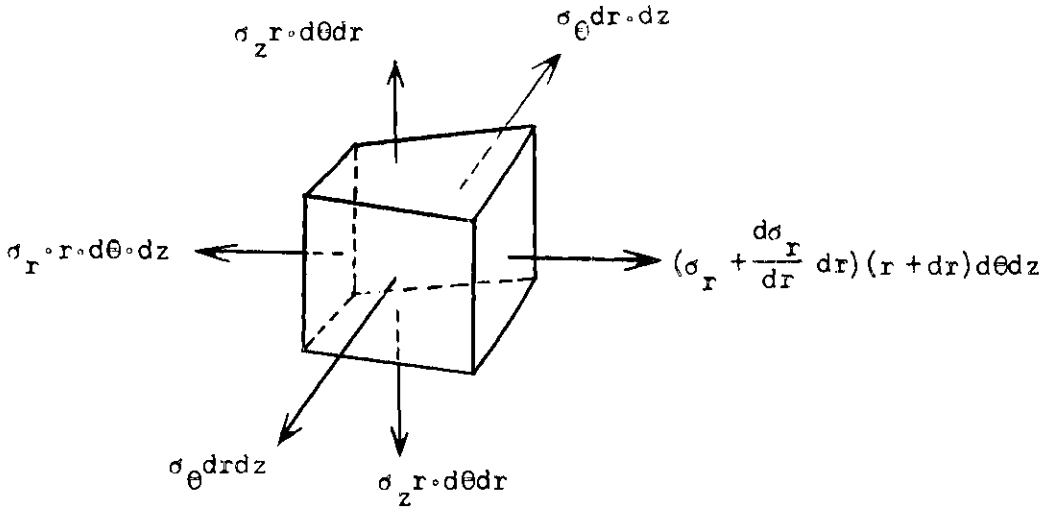

(b) Forces on Volume Element E

Figure 8. Stresses on a Volume Element for a Long Cylinder.

where A is a constant of integration.

At $r = \frac{B}{2}$, $\sigma_r = p_h$

$$\sigma_r = \left[p_h + \frac{2cN_\varphi^{1/2}}{N_\varphi - 1} \right] \left(\frac{r}{B/2}\right)^{\left(\frac{1}{N_\varphi} - 1\right)} - \frac{2cN_\varphi^{1/2}}{N_\varphi - 1} \tag{15}$$

and

$$\sigma_\theta = \left[\frac{p_h}{N_\varphi} + \frac{2c}{N_\varphi^{1/2}(N_\varphi - 1)} \right] \left(\frac{r}{B/2}\right)^{\left(\frac{1}{N_\varphi} - 1\right)} - \frac{2cN_\varphi^{1/2}}{N_\varphi - 1} \tag{16}$$

at $r = \frac{L}{2}$, equating octahedral normal stress with p_o, and using $\sigma_z = \frac{1}{2}(\sigma_r + \sigma_\theta)$

$$p_o = \left(\frac{p_h}{2} + \frac{cN_\varphi^{1/2}}{N_\varphi - 1}\right)\left(\frac{L}{B}\right)^{\left(\frac{1}{N_\varphi} - 1\right)}\left(\frac{1}{N_\varphi} + 1\right) - \frac{2cN_\varphi^{1/2}}{N_\varphi - 1} \tag{17}$$

solving for p_h and using

$$p_h = \frac{q_o}{N_\varphi} - \frac{2c}{N_\varphi^{1/2}} \tag{18}$$

$$q_o = p_o \frac{2N_\varphi^2}{1 + N_\varphi}\left(\frac{L}{B}\right)^{\left(1 - \frac{1}{N_\varphi}\right)} + c\left[N_\varphi \cot\varphi \left\{\left(\frac{2N_\varphi}{1 + N_\varphi}\right)\left(\frac{L}{B}\right)^{\left(1 - \frac{1}{N_\varphi}\right)} - 1\right\} + 2N_\varphi^{1/2}\right]$$

$$q_o = cR_c + p_o R_p \tag{19}$$

where R_c and R_p are dimensionless factors and

$$R_p = \frac{2N_\varphi^2}{1 + N_\varphi} \left(\frac{L}{B}\right)^{\left(1 - \frac{1}{N_\varphi}\right)} \tag{20}$$

and

$$R_c = (R_p - N_\varphi)\cot\varphi + 2N_\varphi^{1/2} \tag{21}$$

(b) For very thin blocks, with low $\frac{H}{B}$ ratios.

As the tube or thin cylinder is very short, the longitudinal stress is zero for all points or $\sigma_z = 0$, and the tube is in a plane-stress condition (Figure 9). The condition of plasticity according to Sach's and Lubahn (24) becomes

$$\sigma_r^2 - \sigma_r \cdot \sigma_\theta + \sigma_\theta^2 = p_t^2 \tag{22}$$

where σ_r and σ_θ are the radial and tangential stresses and p_t is the tensile strength of the material or

$$\sigma_\theta = \frac{1}{2}\left(\sigma_r + \sqrt{4p_t^2 - 3\sigma_r^2}\right)$$

The differential equation of equilibrium is

$$\frac{d\sigma_r}{dr} + \frac{\sigma_r - \sigma_\theta}{r} = 0 \tag{23}$$

Solving equations (22) and (23) gives

$$\log_e \frac{r}{L/2} = \frac{\sqrt{3}}{2} \sin^{-1}\left(\frac{\sqrt{3}}{2}\frac{\sigma_r}{p_t}\right) - \frac{1}{2}\log_e\left(\sqrt{1 - \frac{3}{4}\frac{\sigma_r^2}{p_t^2}} - \frac{\sigma_r}{2p_t}\right) \tag{24}$$

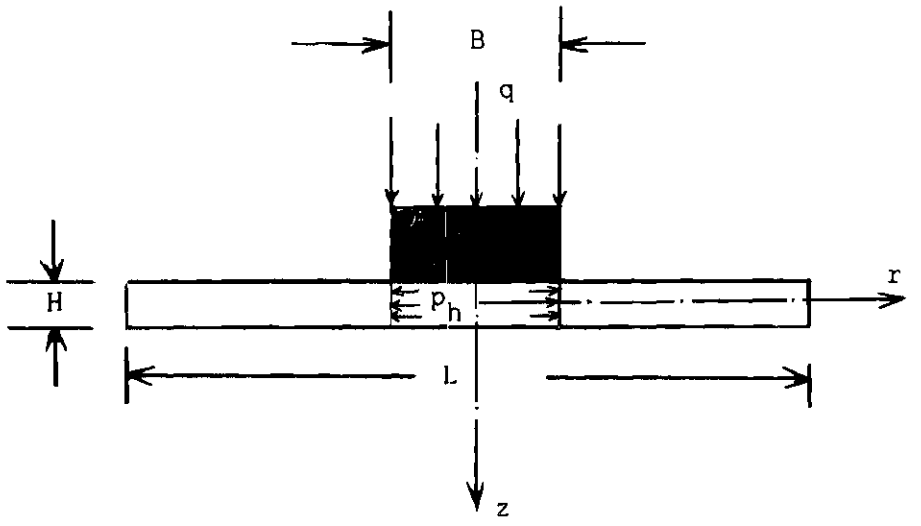

Figure 9. Analysis of the Bearing Capacity of Circular Footings on Jointed System with Low $\frac{H}{B}$ Ratios.

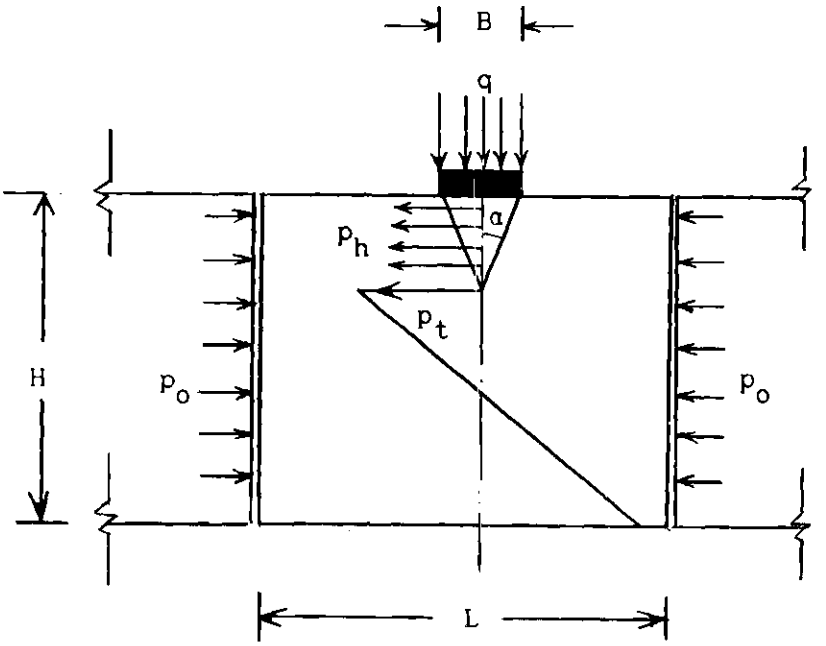

Figure 10. Analysis of the Bearing Capacity of a Strip Footing for a Closed Jointed Rock System.

or

$$\frac{r}{L/2} = \frac{e^{\frac{\sqrt{3}}{2}\sin^{-1}\left(\frac{\sqrt{3}}{2}\frac{\sigma_r}{p_t}\right)}}{\left\{\left(1 - \frac{3\sigma_r^2}{4p_t^2}\right) - \frac{\sigma_r}{2p_t}\right\}^{\frac{1}{2}}}$$

At $r = B/2$, $\sigma_r = p_h$ or

$$\frac{B}{L} = \frac{e^{\frac{\sqrt{3}}{2}\sin^{-1}\left(\frac{\sqrt{3}}{2} - \frac{p_h}{p_t}\right)}}{\left\{\left(1 - \frac{3}{4}\frac{p_h^2}{p_t^2}\right) + \frac{p_h}{2p_t}\right\}^{1/2}} \qquad (25)$$

Solving for p_h and using

$$p_h = \frac{q_o}{N_\varphi} - \frac{2c}{N_\varphi^{1/2}} \qquad (26)$$

Solving equations (25) and (26) gives

$$q_o = 2cN_\varphi^{1/2} + \frac{2}{\sqrt{3}} N_\varphi \sin\left[\frac{2}{\sqrt{3}}\log_e\left(\frac{B}{L}\right) + \frac{1}{\sqrt{3}}\log_e\left[\left(1 - \frac{3}{4p_t^2}\left\{\frac{q_o}{N_\varphi} - \frac{2c}{N_\varphi^{1/2}}\right\}\right)^{1/2} + \frac{1}{2p_t}\left\{\frac{q_o}{N_\varphi} - \frac{2c}{N_\varphi^{1/2}}\right\}\right]\right] \qquad (27)$$

Equation (27) gives the bearing capacity of a circular footing resting on thin blocks of the jointed system. Also the values of R_p and R_c have

been provided in the form of charts (Figure 20, 21) with varying ratio of block width to footing width. Thus knowing the value of the cohesion and angle of internal friction of rock, c and φ, the confinement on the rock block and the ratio of the block width and thickness, to the footing width, the bearing capacity of a circular footing resting on a jointed rock system can be easily estimated with the help of the charts and using equations (19) and (27). The results obtained by using equations (19) and (27) and the charts are discussed in Chapters VI and VII.

A complete theoretical analysis for other shapes of footings was not possible due to the complications involved in using different shapes and emperical shape factors have been suggested for the strip and square footings in this investigation based on the experimental results. The details of the shape factors suggested are given in Chapter VII.

Modification of Meyerhof Theory for Closed Jointed System

It should be noted that the equation developed below, and the original Meyerhof equation have been used for comparison purposes only, as the results obtained by using these equations fail to agree with the experimental results in this investigation, the details of which are given in Chapter VII.

Meyerhof (2) gave the bearing capacity of a strip footing resting on a block of thickness H and width $L \geq H$ as

$$q_o = \frac{(\frac{2H}{B} - \cot\alpha)^2 \cot\alpha\, p_t}{\frac{8H}{B} - \cot\alpha} + 2c\cot\alpha \qquad (28)$$

The rock block shown in Figure 10 is confined by a confining pressure

of p_o. At the bearing capacity q_o of a strip footing of width B, resting on a block of thickness H and width $L \geq H$, the horizontal splitting pressure p_h in accordance with Mohr-Coulomb theory is:

$$p_h = q_o \tan^2\alpha - 2c \tan\alpha \tag{29}$$

whose resultant acts at a depth of $\frac{B}{4}\cot\alpha$, where the semi-wedge angle $\alpha = 45° - \frac{\varphi}{2}$. The maximum tensile stress at the point of the wedge of the material below the footing caused by splitting pressures p_h and confining pressures p_o can be shown to be

$$p_t = p_t' - p_t'' \tag{30}$$

where p_t' and p_t'' can be calculated by taking resultants of p_h and p_o as eccentric loads, acting only on the part of block below the wedge. This will create tension below the wedge and compression on the bottom part of the block.

$$p_t' = \frac{p_h \frac{B}{2}\cot\alpha}{H - \frac{B}{2}\cot\alpha}\left(1 + \frac{3H}{H - \frac{B}{2}\cot\alpha}\right) \tag{31}$$

and,

$$p_t'' = \frac{p_o \times H}{H - \frac{B}{2}\cot\alpha}\left(1 + \frac{3\frac{B}{2}\cot\alpha}{H - \frac{B}{2}\cot\alpha}\right). \tag{32}$$

Putting values of p_t' and p_t'' in equation (30) and solving for q_o using the value of p_h from equation (29), the bearing capacity for a closed

jointed system is given by

$$q_o = \frac{\cot \alpha}{\frac{8H}{B} - \cot \alpha} \left[\left(\frac{2H}{B} - \cot \alpha \right)^2 p_t + \frac{4 p_o H}{B} \left(\frac{H}{B} - \cot \alpha \right) \right] + 2c \cot \alpha. \quad (33)$$

CHAPTER VI

RESULTS

Triaxial Tests

The stress and strain calculations for all the rock samples tested in the triaxial cell, in order to find the strength parameters c and φ of the rock material used in this investigation, were plotted for each test. All the curves indicate an elastic deformation, upon initial loading up to a limiting stress level. Cn some of the curves, this limiting or yield stress is clearly defined and rupture takes place almost immediately after it is reached.

The maximum deviator stress is reached at the failure, thus a peak strength is reached and the sample fractures. The maximum deviator stress is defined as the difference between the principal stresses at failure, that is $(\sigma_1 - \sigma_3)$. The maximum shear stress applied to the rock specimens during these tests is equal to one-half the maximum deviator stress or,

$$\tau_{max} = \frac{1}{2} (\sigma_1 - \sigma_3)$$

This maximum shear stress is the radius of the Mohr Circle, the center of the stress circle is located at $\frac{1}{2}(\sigma_1 + \sigma_3)$ on the axis. Mohr diagrams for the samples tested are presented by Figure 12. The plotted circles are for the averaged values from the entire series, which consists of four test specimens for each confinement pressure. Typical stress-strain curves for the rock samples tested are shown in Figure 11. The

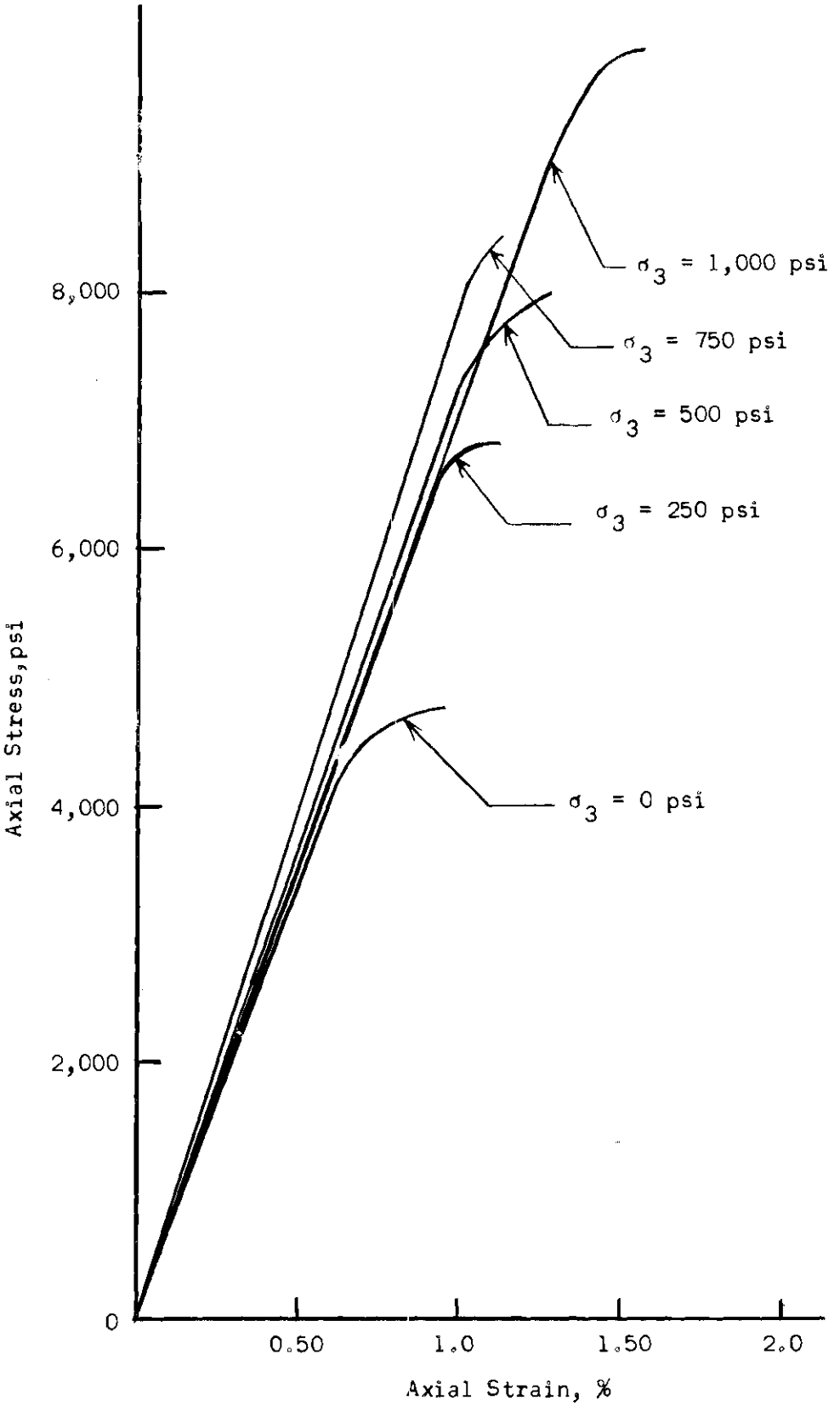

Figure 11. Typical Axial Stress-Strain Curves for Indiana Limestone.

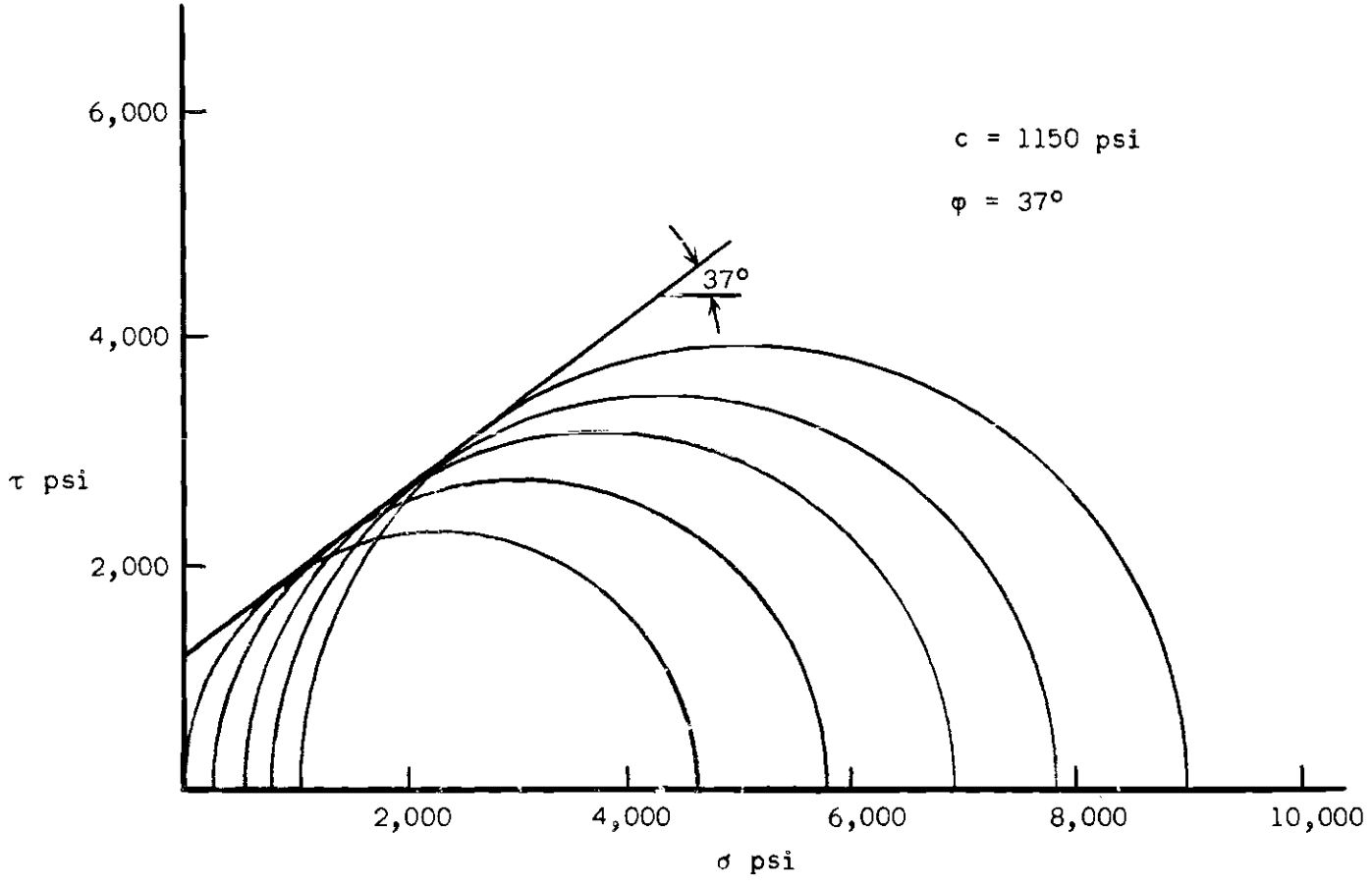

Figure 12. Mohr's Circles for Indiana Limestone Using Triaxial Cell Test Results.

strength results of the test conducted are listed in Table 1.

On the basis of these data, a Mohr failure envelope can be determined. The limiting stress condition at a point are represented by the Mohr stress circle. Each set of principal stresses has a unique circle which is defined by the minor principal stress (confining pressure) and the deviator stress. For a given confining pressure the value of the deviator stress was taken as the average value of the maximum deviator stress of all the samples tested with that confining pressure. With these deviator stresses, a set of circles is drawn. According to Mohr, the envelope of the circles is the critical stress function. The envelope, a straight line under the range of confining pressures used in this investigation can be represented by the equation

$$\tau = c + \sigma_n \tan \varphi \ .$$

where c is termed as the cohesion and φ as the angle of internal friction of the material. The value of c, obtained in this manner, for the rock material used in this investigation is 1150 psi, and the value of φ is 37°. The variation of the radius of the Mohr Circle $\frac{1}{2}(\sigma_1 - \sigma_3)$ is a function of the distance from the σ, τ origin to the center of the circle that is $\frac{1}{2}(\sigma_1 + \sigma_3)$. The results of this investigation are presented in this form in Figure 13 and in form of Table 2. The slope of the line in this plot is 31°, thus showing Tan δ = Sin φ for the samples tested.

The condition of rock samples after testing can be clearly seen through the plastic membrane. A single distinct failure plane was observed for each sample tested. For a comparison the test results of this investigation are given below with the earlier work done on limestone by other investigators.

Table 1. Triaxial Cell Test Results

Test No.	Cell Pr. psi	Stresses at Failure σ_1 psi	σ_2 psi	σ_3 psi	σ_o psi	τ_o psi	e_{Strain}
RTC-2	1000	9049	1000	1000	3284	3229	.019
RTC-3	1000	9344	1000	1000	3398	3390	.017
RTC-4	1000	8973	1000	1000	3684	3794	.016
RTC-5	1000	8526	1000	1000	3397	3388	.018
RTC-6	750	8153	750	750	2931	3084	.029
RTC-7	750	7406	750	750	2941	3096	.020
RTC-8	750	8141	750	750	2681	2729	.019
RTC-9	750	6864	750	750	3116	3345	.019
RTC-10	500	7107	500	500	2247	2469	.016
RTC-11	500	7107	500	500	2413	2705	.014
RTC-12	500	6453	500	500	2522	2858	.015
RTC-13	500	6923	500	500	2406	2695	.018
RTC-14	250	4746	250	250	1537	1820	.012
RTC-15	250	6037	250	250	2180	2728	.014
RTC-16	250	6682	250	250	2395	3032	.012
RTC-17	250	5910	250	250	1906	2340	.021
RTC-18	0	3709	0	0	1237	1749	.009
RTC-19	0	4626	0	0	1542	2181	.007
RTC-21	0	5592	0	0	1865	2636	.008
RTC-22	0	4357	0	0	1458	2054	.015

Table 2. Principal Stress Difference vs. Principal Stress Sum Values at Failure for Triaxial Cell Tests for Indiana Limestone

Test No.	Cell Pressure psi	$\frac{\sigma_2}{\sigma_1}$	$\sigma_1 - \sigma_3$ psi	$\sigma_1 + \sigma_3$ psi
RTC-2	1,000	0.111	8049	10,049
RTC-3	1,000	0.107	8344	10,344
RTC-4	1,000	0.111	7972	9,972
RTC-5	1,000	0.117	7525	9,525
RTC-6	750	0.092	7403	8,903
RTC-7	750	0.102	6570	8,070
RTC-8	750	0.101	6656	8,156
RTC-9	750	0.092	7311	8,891
RTC-10	500	0.072	6414	7,414
RTC-11	500	0.070	6608	7,608
RTC-12	500	0.076	6063	7,063
RTC-13	500	0.072	6423	7,423
RTC-14	250	0.053	4416	4,996
RTC-15	250	0.041	5788	6,288
RTC-16	250	0.037	6432	6,932
RTC-17	250	0.042	5661	6,161
RTC-18	0	0	3709	3,709
RTC-19	0	0	4626	4,626
RTC-21	0	0	5592	5,592
RTC-22	0	0	4357	4,357

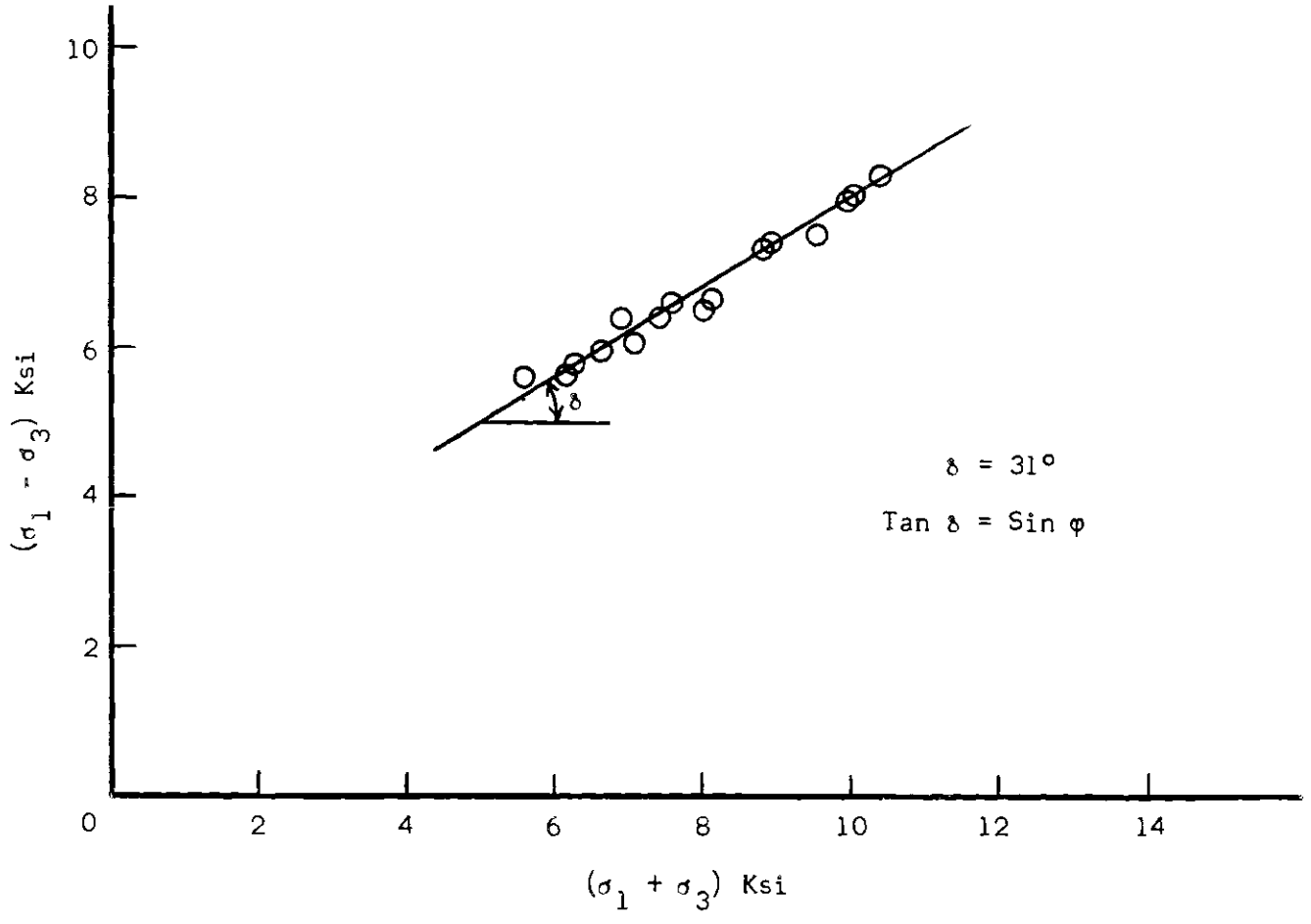

Figure 13. Principal Stress Difference vs. Principal Stress Sum at Failure for Indiana Limestone.

Investigator	Value	Cohesion psi	p_t psi
Schwartz	46°	1100	392
Mazanti	35.1°	1740	-
Johnson	37°	910	410
Present Investigator	37°	1150	420

Plane Strain Tests

The results of plane strain tests are shown in Table 3. The Mohr circles obtained using these results are shown in Figure 14. The value of φ' obtained from Mohr's envelope is 39.6°. There seems to be an increase of φ value of about 2.6°, which is about seven percent increase in the value obtained in Triaxial tests. Also $(\sigma_1 - \sigma_3)$ values are plotted against $(\sigma_1 + \sigma_3)$ values for the tests conducted. The slope of the envelope, shown in Figure 15 is found to be 32.5°. Thus the value of tan δ' is equal to Sin φ'. Table 3 presents the principal stress difference, principal stress sum and their ratio for the tests done in this investigation.

Bearing Capacity Results

An open jointed system will be referred to here as "a jointed rock system in which the blocks adjoining the loaded blocks will have negligible or no effect on the bearing capacity of the loaded blocks" whereas, "in a closed jointed system the adjoining blocks will have a significant effect on the bearing capacity of the loaded blocks." Due to the confinement produced by the adjoining blocks on the loaded blocks the bearing capacity of the loaded blocks will be increased in a closed jointed system.

Table 3. Plane Strain Test Results, Stresses at Failure for Indiana Limestone

Test No.	σ_1 psi	σ_2 psi	σ_3 psi	$\frac{\sigma_2}{\sigma_1}$	$\sigma_1 - \sigma_3$ psi	$\sigma_1 + \sigma_3$ psi	σ_o psi	τ_o psi
RPS-1	9488	2394	1000	0.252	8488	10,488	4298	3116
RPS-2	9242	1863	1000	0.202	8242	10,242	4036	3698
RPS-3	9627	2114	1005	0.220	8622	10,632	4250	3829
RPS-4	8390	1681	750	0.200	7640	9140	3608	3403
RPS-5	8168	1894	750	0.232	7418	8118	3605	3261
RPS-6	7222	1444	500	0.200	6722	7722	3056	2971
RPS-7	7268	1456	500	0.200	6768	7768	3075	2990
RPS-8	6849	1241	480	0.181	6367	7327	2857	2839
RPS-9	6070	1522	250	0.251	5820	6320	2614	2498
RPS-10	5897	1077	250	0.183	5647	6147	2409	2490
RPS-11	4654	849	0	0.182	4654	4654	1835	2024
RPS-12	4901	888	0	0.181	4901	4901	1930	2132
RPS-13	5331	1013	0	0.190	5331	5331	2115	2312

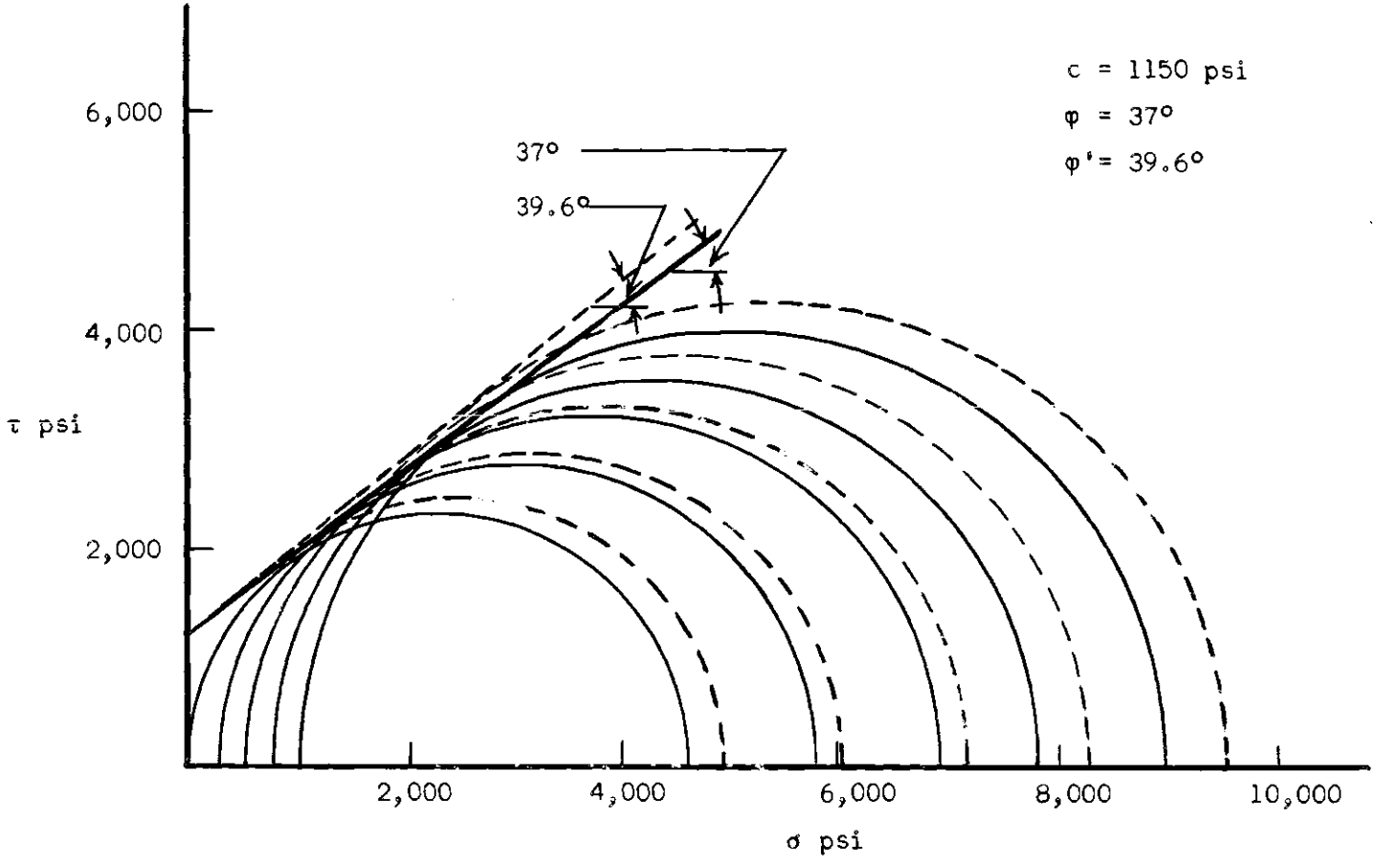

Figure 14. Mohr's Circles for Indiana Limestone Using Plane Strain Test Results.

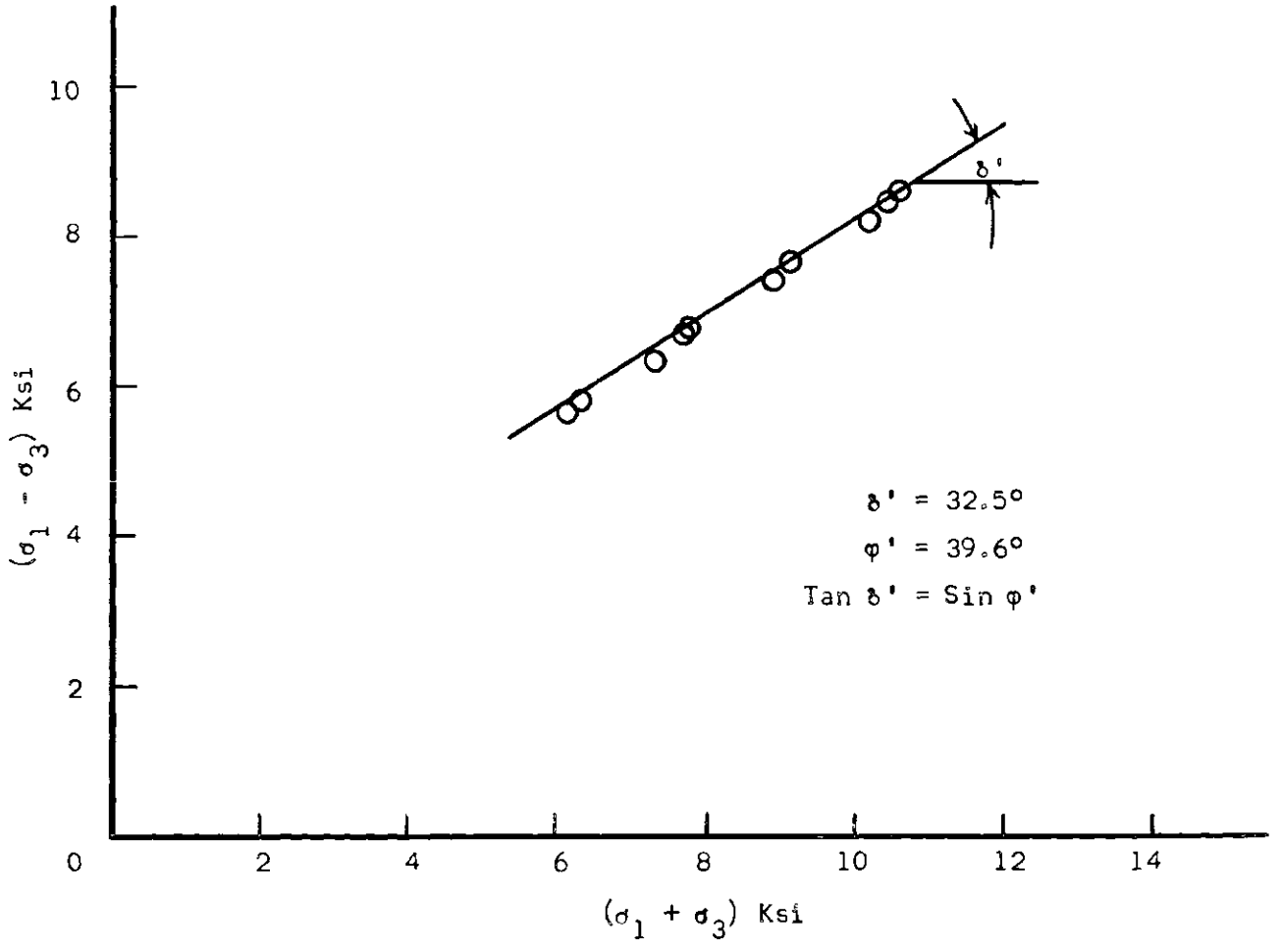

Figure 15. Principal Stress Difference vs. Principal Stress Sum for Plane Strain Tests at Failure for Indiana Limestone.

When the load was applied to the footings, an initial settlement of the system took place at much lower loads, and after this settlement, the model footing load began to build up at a rate more rapid than in the beginning phase of the testing. In most of the tests the load settlement curves assumed a flatter, constant slope at this point (Figures 17 and 18).

In most of the cases, the initial settlement of the system was complete when the magnitude of the load on the footing was between one to ten percent of the total failure load, and after this the load began to build up at a faster rate. The change in the slope of the load vs. settlement curves usually occurred at settlements ranging from 0.02 to 0.05 inch, and most frequently the readings were closer to the former one.

At failure, there was usually a decline in the rate of load, Figures 17 and 18. As failure was approached, the model footing load would reach a maximum value and stay at that value for a very short period of time, while the deformation continued. It was usually followed by an increased rate of settlement and failure. In cases of open jointed system, the load dropped sharply after failure to values of 60 to 75 percent of the failure load in most of the cases, Figure 17. In case of a closed jointed system, the failure was clearly marked, on the load settlement curve by a drop in the load by 15 to 20 percent (Figure 18), but if the deformation was continued afterwards, the load rose again to the failure value and then afterwards the load settlement curve took a constant slope, the load constantly increasing with the deformation, Figure 18. The slope of the curve after failure was much steeper than the original slope before failure in almost every case, indicating that the load increment varied

much less with deformation after failure compared to deformation before failure.

In most of the cases for both the open jointed and the closed jointed system, only the central column of blocks which were loaded failed, and adjoining blocks were not much affected (Figure 16a). In a few cases of closed jointed system, the radial failure cracks were also extended to the adjoining blocks. In some tests of closed jointed system, it was noted that the cracks in the adjoining blocks were hair-thin and could not be easily observed. But if the deformation was continued after failure, the cracks widened and could be very clearly seen.

In open jointed system, the strain gauge indicators indicated no load transfer or negligible amount in all the tests before the failure was reached. However, if deformations were continued after failure was reached, there was a little lateral load transferred on the sides, depending upon the deformations experienced after failure. Thus p_o was taken to be zero in case of open jointed system for the calculations of the bearing capacity.

In case of closed jointed system the blocks were already confined together before the start of the test. In this case, the lateral pressure on the sides of the box increased during testing. The increase in pressure in most of the tests was between 5 to 10 percent of the original confinement used on the side of the box, prior to failure. After failure there was a significant and sudden increase of the lateral pressure on the sides of the box. The pressure increased with the increase in deformation after failure in most of the tests on closed jointed systems. Thus in tests on closed jointed systems a confining pressure was used for the

system when calculating the theoretical bearing capacity. Some of the typical load settlement curves both for open jointed system and closed jointed systems are shown in Figures 17 and 18.

The results of the tests conducted on circular footings for open jointed system are given in Tables 4 and 10 to 15, and for closed jointed system are given in Tables 5 and 16 to 20.

For strip footings the result of open jointed system are given in Tables 6, and 21 to 23, and for closed jointed system in Tables 7 and 24.

Square footing test results are shown in Tables 8, 25 and 26, for open jointed system and in Tables 9 and 27 to 29 for closed jointed system.

CHAPTER VII

DISCUSSION OF RESULTS AND CONCLUSIONS

Initial Settlement

Load settlement curves were plotted for the bearing capacity tests conducted in this investigation both for open and closed jointed systems. As mentioned in the previous chapter, in all the tests for open and closed jointed systems, an initial settlement of the system takes place, when the load is applied to the footings. This settlement is about one per cent of the height of the system. The amount is equivalent to the sum of the block tolerances for the flatness, 0.015 inch per block. Thus the initial settlement appears to take place due to the adjustment of the blocks over the irregularities and small gaps left between the blocks due to horizontal joints. Due to this initial settlement, the load settlement curves have a very steep slope in the beginning of the test, which gives them the shape shown in the load settlement curves (Figures 17 and 18). With the initial settlement the majority of the separations occurring in a horizontal plane between the stacked blocks seem to close, as after this the load settlement curve assumes a flatter, constant slope.

For all shapes of footings and for both jointed systems, the load settlement curves seem to be quite similar in shape prior to failure. However, after failure, which is distinctly marked in all the tests by a drop in rate of loading after a peak value, the behavior is different in the two cases of open and closed jointed systems.

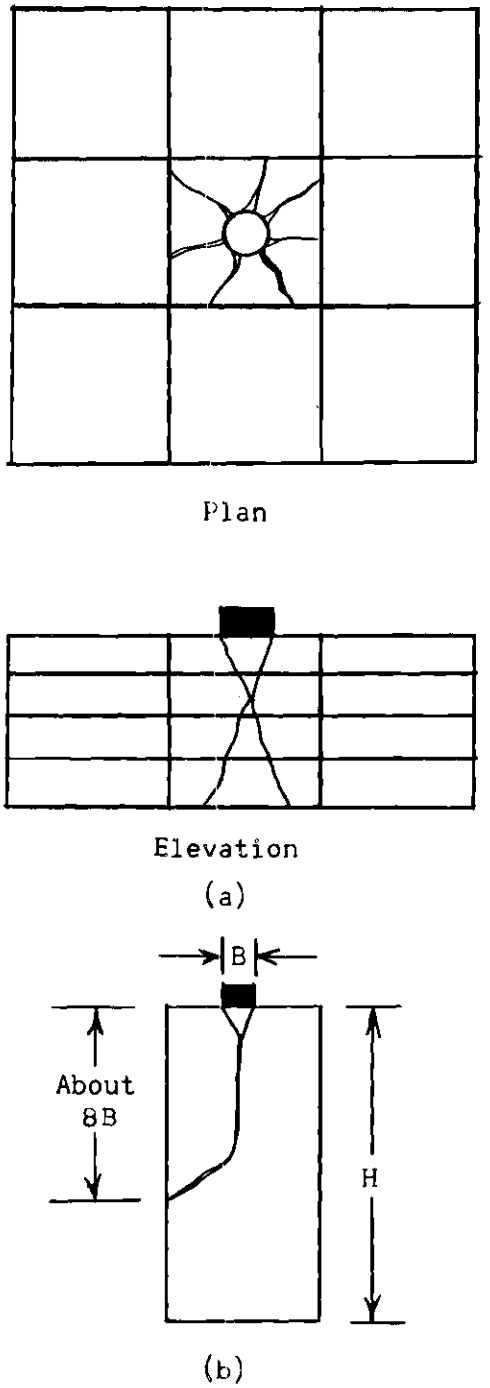

Figure 16. (a) Typical Failure Crack Pattern for Jointed Rock System with $\frac{H}{B}$ Less than about Eight.
(b) Typical Failure of Loaded Blocks with $\frac{H}{B}$ More than about Eight.

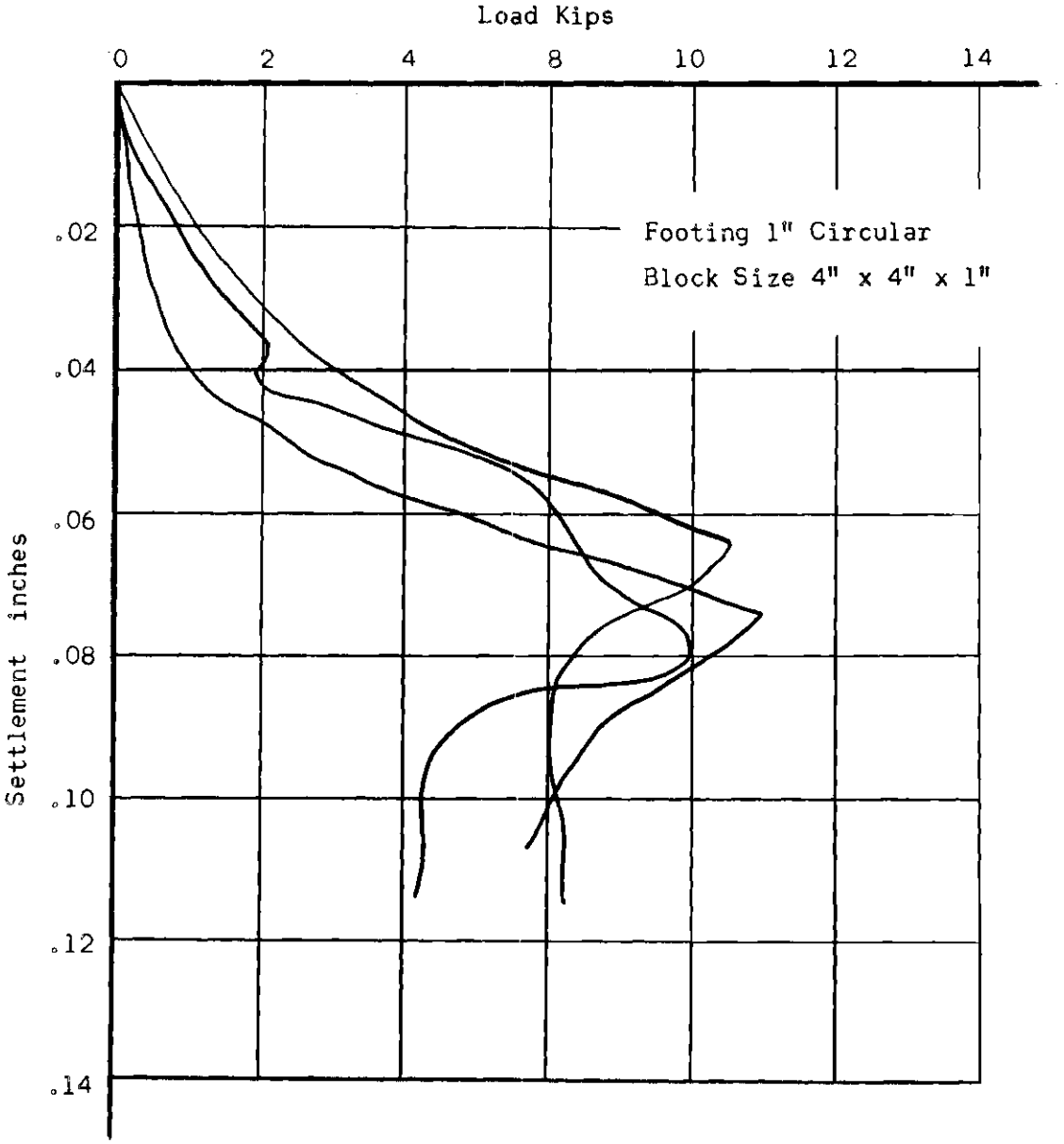

Figure 17. Typical Load Settlement Curves for 1" Circular Footings on 4" x 4" x 1" Blocks. (Open Jointed System)

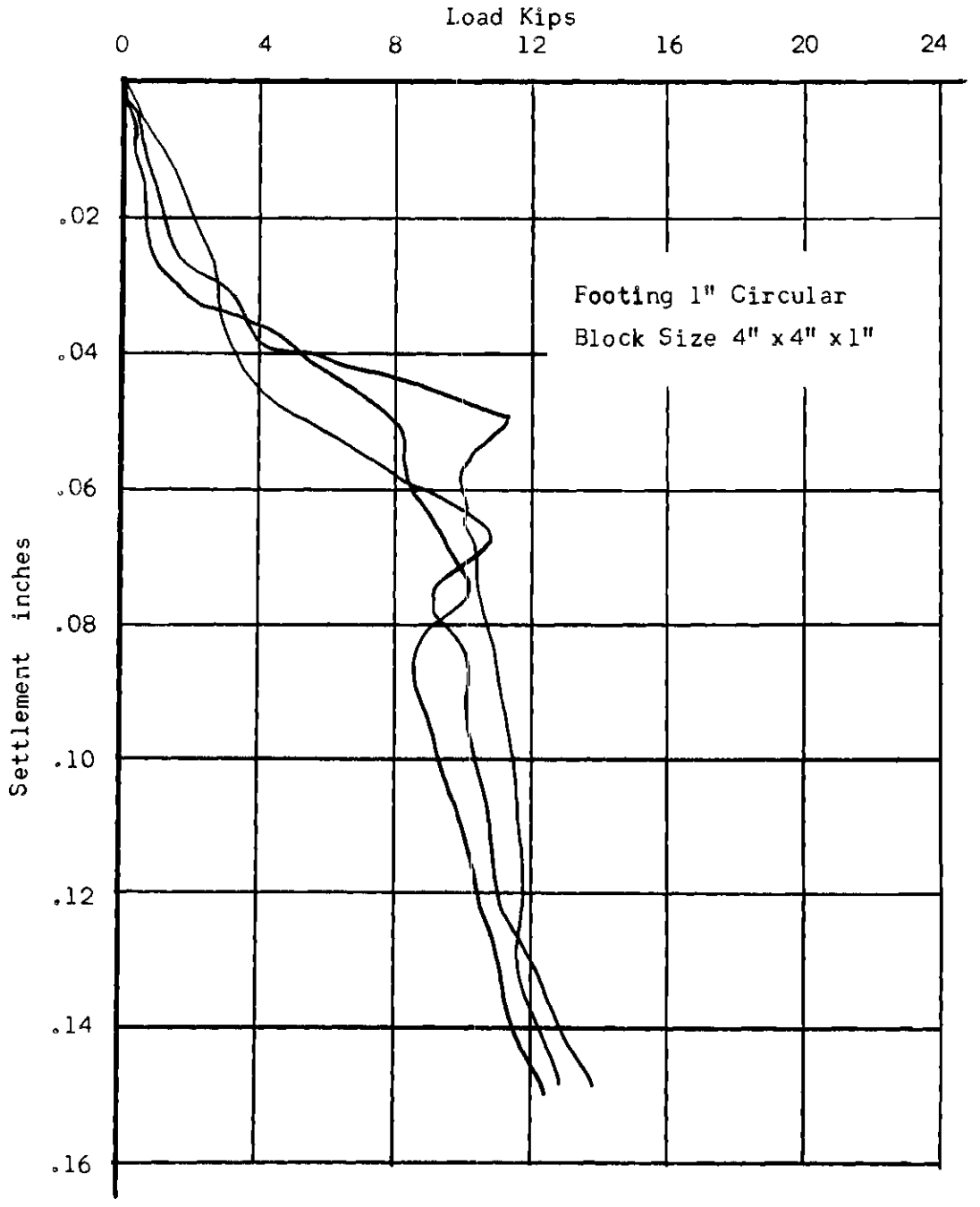

Figure 18. Typical Load Settlement Curves for 1" Circular Footing on 4" x4" x1" Blocks. (Closed Jointed System)

In a closed jointed system there was again an increase in the load after failure, if the deformation was continued. This increase in the load is probably due to the sharp increase in the confinement produced by the sides of the box on the system after failure. The confinement pressure seems to be produced by the wedging of the material horizontally by the footing wedge formed immediately below the footing at failure. Below the results are discussed under separate headings for the different shapes of footings tested in this investigation.

Circular Footings

The bearing capacity was first theoretically calculated using equation (19). As stated in the chapter, theoretical development, the theoretical derivation was obtained for an expanding cylinder, to be used for bearing capacity of circular footings. For the ratios of $\frac{H}{B} > 8$ the experimental results agree with the theoretical equation (19), as the blocks in this case seem to behave as a long cylinder (Figure 19). Experiments done on blocks having $\frac{H}{B} > 8$ show that the bearing capacity does not increase with increasing $\frac{H}{B}$ ratio more than about eight. This is due to the type of failure for such blocks with $\frac{H}{B}$ ratio greater than about eight as shown in Figure 16b.

Due to the axial restraint in a long cylinder the pressure required for expansion failure will be higher for this case, than in the case of a short one. Thus, for low values of $\frac{H}{B}$ the experimental value of bearing capacity should be less than the theoretical value for the infinitely long cylinder. This was found to be true, as shown in Figure 19. The value reduces with the reduction of $\frac{H}{B}$ ratio. For $\frac{H}{B}$ values of $\frac{1}{12}$ to $\frac{1}{2}$, the

experimental results agree with the theoretical equation (27), for a short cylinder, Figure 19. For the values of $\frac{H}{B}$ between $\frac{1}{2}$ and 8, there is a transition between the two limits. The experimental data available was examined, Figure 19, and a factor J was obtained to take care of the cases in which the ratio $\frac{H}{B}$ was between $\frac{1}{2}$ and 8. The ratio of the experimental bearing capacity of the footing to the theoretical value obtained by using equation (19), is taken here as the J value. The values of J plotted against $\frac{H}{B}$ is shown in Figure 19. The equation of this curve is found to be

$$J = 0.53 \left(\frac{H}{B}\right)^{0.346} \quad \text{for} \quad \frac{1}{2} \leq \frac{H}{B} \leq 8$$

and (34)

$$J = 1 \quad \text{for} \quad \frac{H}{B} > 8$$

for $\frac{H}{B}$ values of $\frac{1}{12}$ to $\frac{1}{2}$, the J value for $\frac{H}{B} = \frac{1}{2}$ can be used.

The equation (19) was modified by multiplying Factor J and the equation for a circular footing resting on a rock block is obtained as follows:

$$q_c = J(cR_c + p_o R_p) \tag{35}$$

where R_c and R_p can be obtained by using equations (20) and (21) or can be found out with the help of charts (20, 21). The value of J can be found from equation (34) or Figure 19 can be used for this purpose.

The experimental results of Meyerhof (2) performed on concrete blocks are also plotted in Figure 19. The results seem to agree with the behavior presented by this graph. The variation in Meyerhof's

Table 4. Bearing Capacity Test Results for Circular Footings on Open Jointed Rock Systems, p_t = 420 psi

Footing Size (In.)	L/B	H/B	Size of Blocks: Width 4" Length 4" Thickness 1" — Experimental Q Lbs.				Experimental q (lbs./sq. in)				Theoretical		Failure Settlement (Inches)		
			Q_1	Q_2	Q_3	$Q_{avg.}$	q_1	q_2	q_3	$q_{avg.}$	q_T	Q_T	S1	S2	S3
1	4	1	10,960	10,500	9,980	10,480	13,950	13,380	12,700	13,350	14,010	11,010	.075	.065	.080
2	2	1/2	20,200 18,500	21,300	18,280	19,570	6,430 5,890	6,780	5,820	6,230	6,280	19,750	.120 .085	.087	.112
3	4/3	1/3	37,450	35,420	35,100	35,990	5,300	5,010	4,960	5,090	3,815	27,000	.087	.068	.102
4	1	1/4	58,600	62,200	56,300	59,030	4,670	4,950	4,480	4,710	4,610	58,000	.085	.123	.087

Table 5. Bearing Capacity Test Results for Circular Footings on Closed Jointed Rock System, P_o = 100 psi

Footing Size (In.)	L/B	H/B	Size of Blocks: Width 4" Length 4" Thickness 1"												
			Experimental Q Lbs.				Experimental q (lbs./sq. in.)				Theoretical		Failure Settlement (Inches)		
			Q_1	Q_2	Q_3	$Q_{avg.}$	q_1	q_2	q_3	$q_{avg.}$	q_T	Q_T	S1	S2	S3
1	4	1	11,700	10,660	12,020	11,460	14,900	14,200	15,300	14,600	14,950	11,730	.106	.080	.091
2	2	1/2	23,200	21,560	22,980	22,580	7,380	6,850	7,320	7,180	6,720	21,100	.093	.137	.120
3	4/3	1/3	40,150	41,350	42,100	41,200	5,680	5,850	5,960	5,820	4,090	35,800	.123	.084	.106
4	1	1/4	69,900	68,200	70,100	69,400	5,560	5,430	5,580	5,525	5,013	63,000	.079	.180	.068

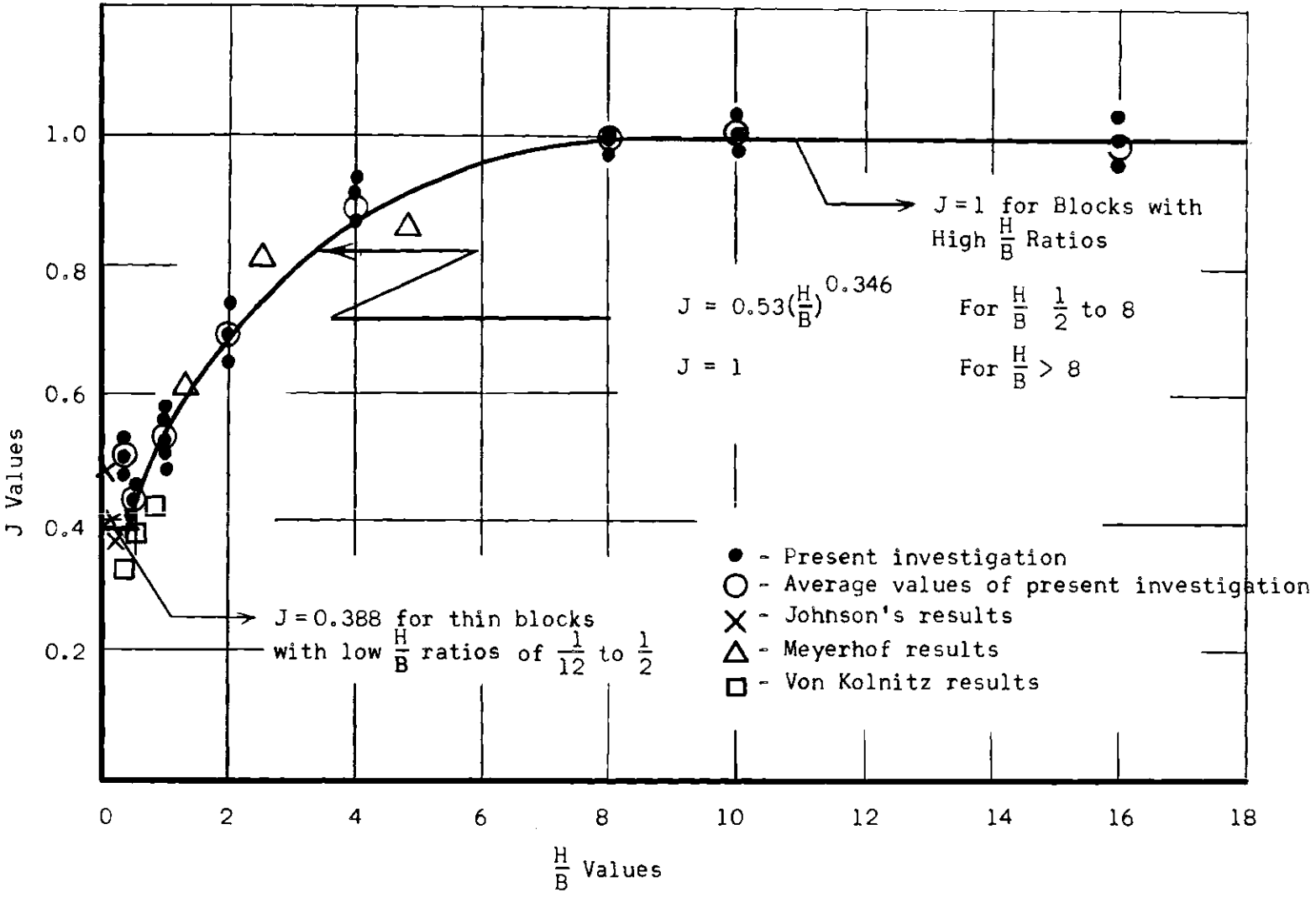

Figure 19. Experimental Results Showing Variation of Bearing Capacity with Ratio of Block Thickness to Footing Width.

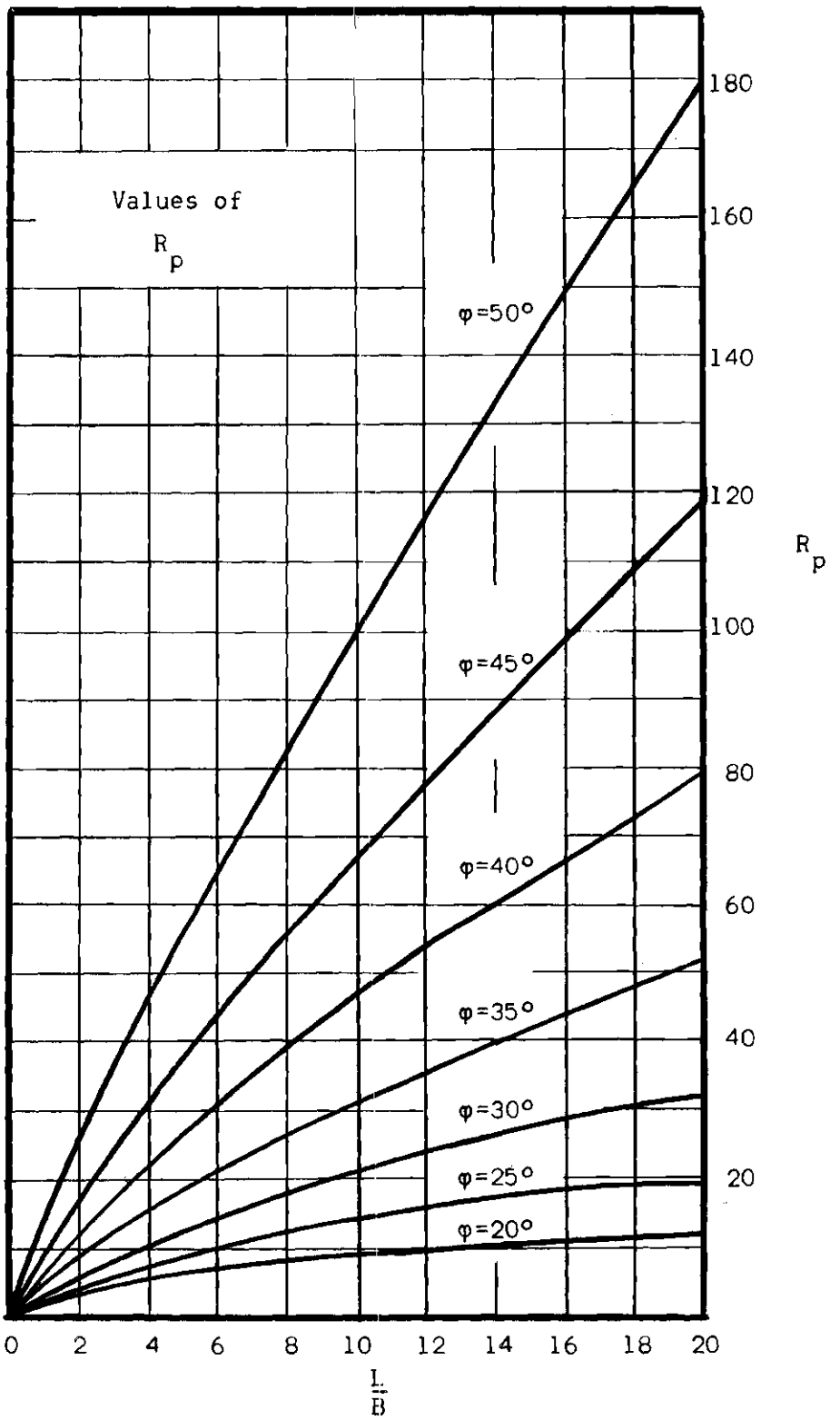

Figure 20. Computed Values of Rock Bearing Capacity Factor R_p, with Angle of Internal Friction φ and $\frac{L}{B}$ Ratio.

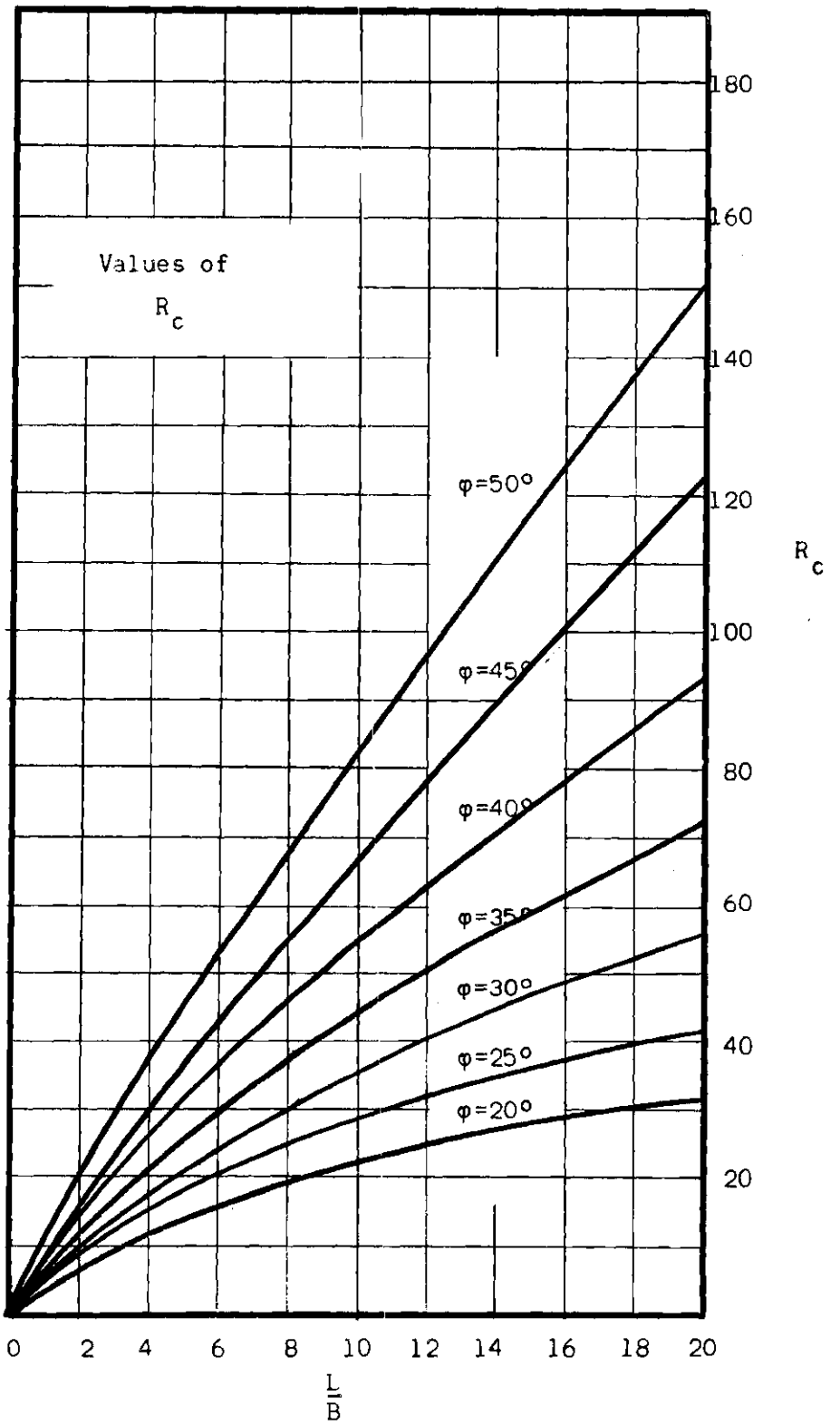

Figure 21. Computed Value of Rock Bearing Capacity Factor R_c, with Angle of Internal Friction φ and $\frac{L}{B}$ Ratio.

results are within 10 per cent of the results of this investigation. Also the experimental results of Von Kolnitz and Johnson are compared with the theoretical results obtained by using the expressions put forward in this investigation and plotted in this figure. The results of blocks of $\frac{H}{B}$ ratios of 1, 1/2, 1/3, and 1/5 seem to be within 10 per cent of the results of this investigation, and agree fairly well to the behavior of the bearing capacity with the change in $\frac{H}{B}$ ratio of the blocks. There is some deviation of about 20 per cent from the theoretical results, in case of some of the experimental results of Johnson for $\frac{H}{B}$ ratio of 1/8 and 1/12. The reason appears to be that in these cases the layers of blocks are very thin in comparison to the width of the footing and failure takes place by crushing of the individual layers, one by one, rather than forming a wedge as in the case of blocks with large thickness.

Thus knowing the strength parameters c and φ and knowing the footing and block dimensions, that is, the value of $\frac{L}{B}$ and $\frac{H}{B}$, the bearing capacity of a circular footing resting on a block of rock can be determined. In the case of open jointed systems the values of p_o have been taken as zero.

Using the confining pressures used in the investigation, 20 and 100 psi, the bearing capacity was calculated for the closed jointed systems using the above equation. The results thus obtained and the experimental results obtained in this investigation are shown in Table 5 and Tables 16 to 18 and in form of plot in Figure 23. The results of the open jointed system are shown in Table 4 and Tables 10 to 15, and in form of plot in Figure 22. The experimental results seem to be in good agreement with the theoretical results, with a maximum variation of about

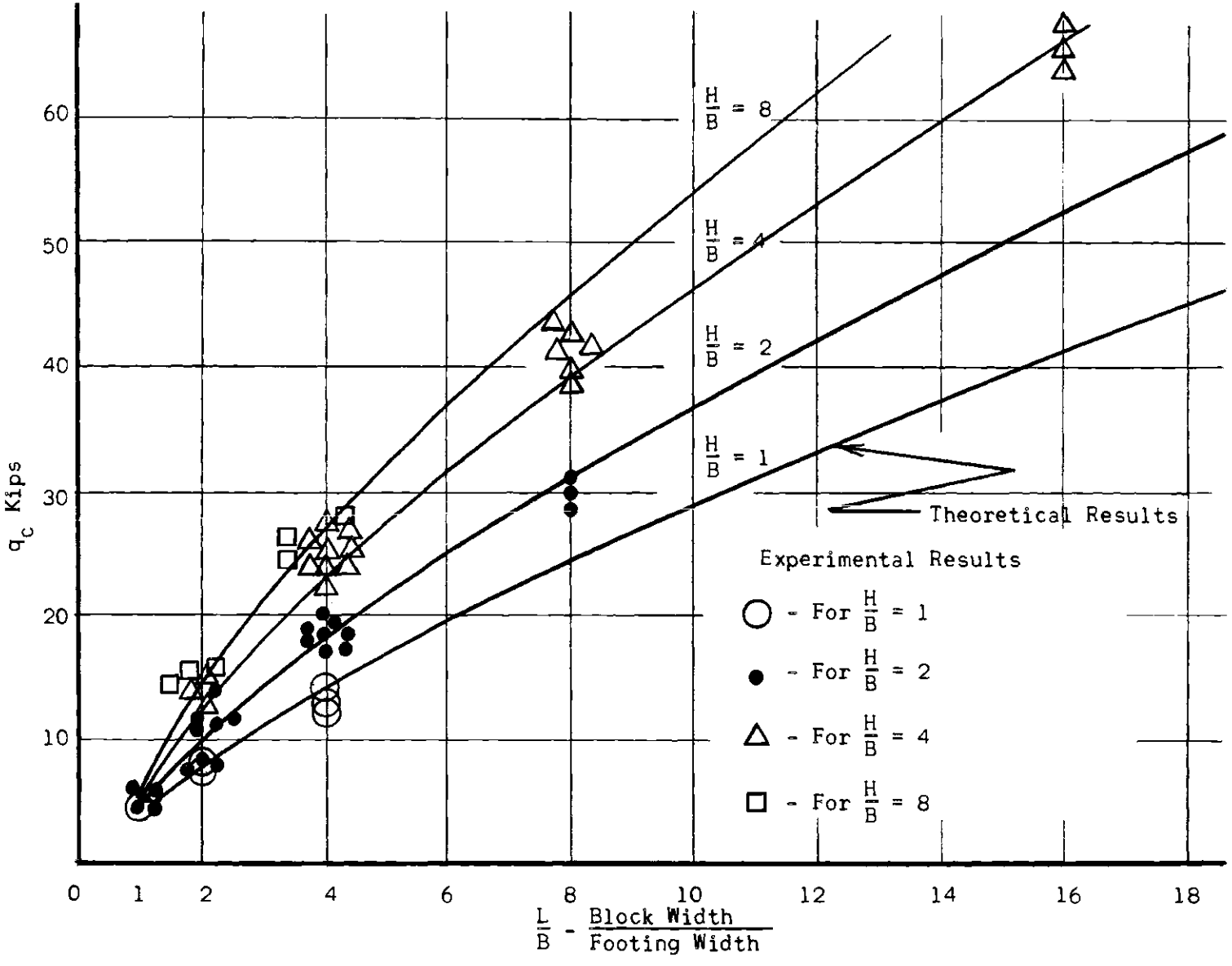

Figure 22. Bearing Capacity of Model Circular Footings on Open Jointed Rock.

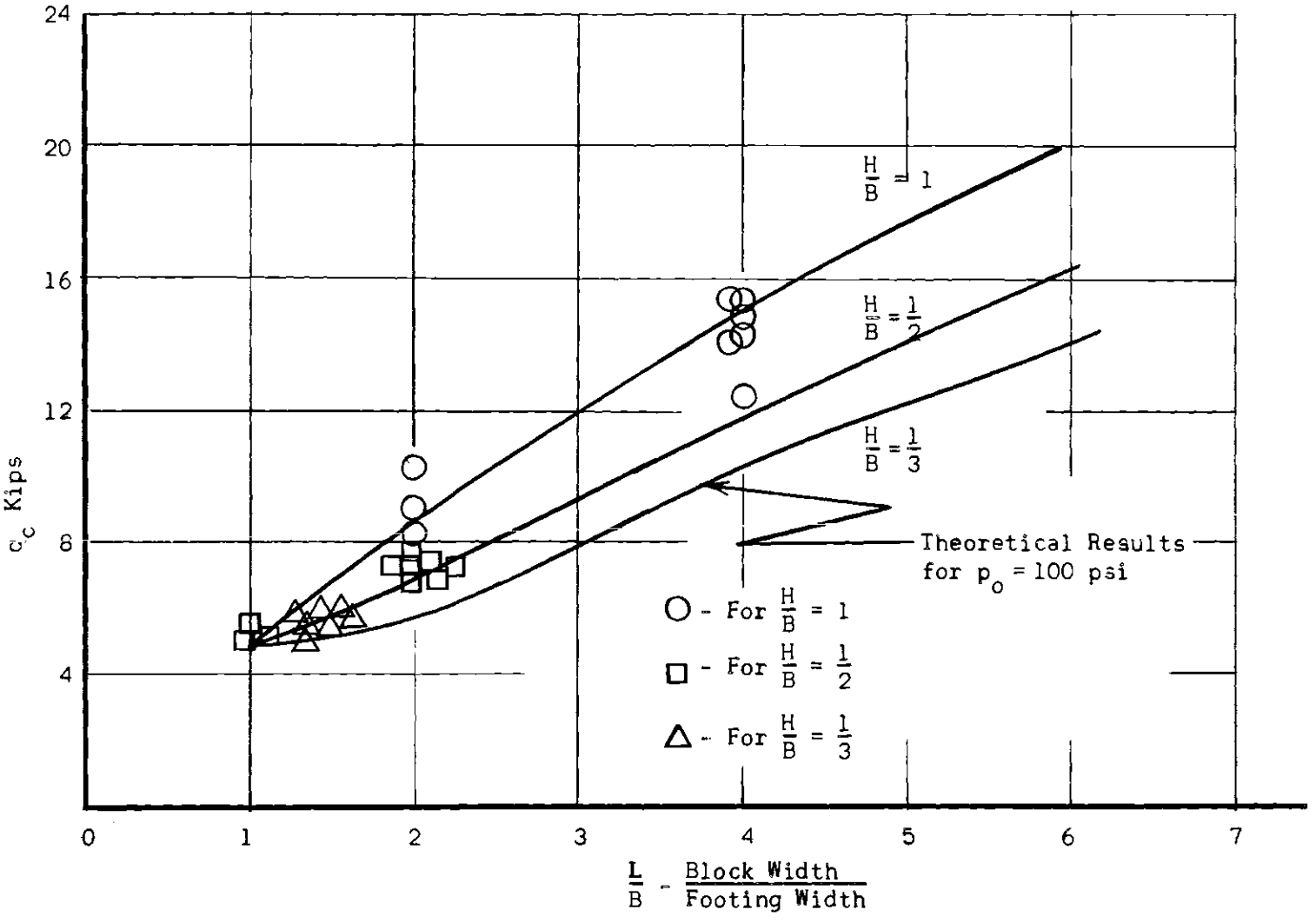

Figure 23. Bearing Capacity of Model Circular Footings on Closed Jointed Rock.

12 per cent.

As a check on the results of closed jointed rock in the box, some tests were performed in the plane strain cell. The results of the bearing capacity tests done in the plane strain cell are shown in Tables 19 and 20. The results show values quite close to those obtained in the aluminum box, for the case of closed jointed systems with maximum deviations of five to seven per cent. However, after failure in this case, the load drops suddenly to very low values as splitting of the blocks takes place and the blocks split away to the sides since there is no adjoining material to check this splitting. Thus the load settlement curves for these tests look very similar to those of the open jointed system, but the failure loads are close to the failure loads for the case of closed jointed systems. Thus, as will be expected, the air pressure is helpful in increasing the failure load of the blocks, but, once the failure load is reached, it is unable to maintain the load at that level or somewhat lower level as in the case of a closed jointed system.

Rectangular Footings

The results of loading tests done on strip footings are given in Tables 6, 7 and 21 to 24, and shown in Figure 24. The square footing test results are in Tables 8, 9 and 25 to 29, and are presented in form of graph in Figure 26. The load settlement curves show a similar behavior, in both cases of open and closed jointed system, as has been discussed earlier in the beginning of this chapter.

Comparison with Meyerhof Theory

For Strip Footings the theoretical results for open jointed system were also calculated by using Meyerhof equation (28) for the sake of

Table 6. Bearing Capacity Test Results for Strip Footings on Open Jointed Rock Systems, p_t = 420 psi

Footing Size (In.)	L/B	H/B	Size of Blocks: (1) Width 3.5" Length 5" Thickness 4"; (2) Width 4" Length 5" Thickness 4" — Experimental Q Lbs.				Experimental q (lbs./sq.in.)				Theoretical		Failure Settlement (Inches)		
			Q_1	Q_2	Q_3	$Q_{avg.}$	q_1	q_2	q_3	$q_{avg.}$	q_T Meyerhof with S	Q_T Meyerhof with S	S1	S2	S3
.35	10	11.5	22,800	26,200	23,300	24,100	13,020	14.950	13,320	13,760	8,510	13,850	.061	.081	.052
.50	8	8	33,600	31,800	33,000	32,800	13,450	12,720	13,200	13,120	7,140	12,800	.056	.062	.035

Table 7. Bearing Capacity Test Results for Strip Footings on Closed Jointed Rock Systems, P_o = 100 psi, p_t = 420 psi

Footing Size (In.)	L/B	H/B	Size of Blocks: (1) Width 3.5" Length 5" Thickness 4"; (2) Width 4" Length 5" Thickness 4" — Experimental Q Lbs.				Experimental q (lbs./sq.in.)				Theoretical		Failure Settlement (Inches)		
			Q_1	Q_2	Q_3	$Q_{avg.}$	q_1	q_2	q_3	$q_{avg.}$	q_T Meyerhof with S Modified	Q_T Meyerhof with S Modified	S1	S2	S3
.35	10	11.5	26,500	29,800	25,600	27,300	15,130	17,010	14,620	15,600	9,475	14,800	.093	.103	.085
.50	8	8	35,800	37,700	36,600	36,700	14,330	15,050	14,620	14,670	7,760	13,650	.081	.076	.106

comparison with the theoretical results obtained by using the expression suggested in this investigation. For the closed jointed system the theoretical results obtained by using the expression suggested in this investigation were compared with the modified equation (33), modified in this investigation along the lines of Meyerhof's original equation (28). Meyerhof suggested the equation (28) for the bearing capacity of blocks having $L \geq H$. In this investigation strip footing tests were also done on blocks with $L < H$. The results of this investigation, along with the investigations of Von Kolnitz (20) and Johnson (21) on square footings are discussed below.

For strip footings calculating the results using Meyerhof equation and comparing the theoretical results with the experimental results, it was found that Meyerhof's equation gives results closer to the experimental ones only in case of tests with $\frac{H}{B} = 11.5$ and $\frac{L}{B} = 4$. For other values used in this investigation, it seems Meyerhof's equation does not agree with the experimental results. For values of $\frac{H}{B}$ of 8 and $\frac{L}{B}$ from 4 to 40 and $\frac{H}{B}$ of 11.5 and $\frac{L}{B}$ of 8 to 40, the experimental results obtained in this investigation fail to agree with the Meyerhof Equation, (Table 6 and Tables 21 to 23, Figure 24). Also, as stated earlier for values of $\frac{H}{B}$ of 1 to 1/4 and $\frac{L}{B}$ values of 1.3 to 3 in the investigation done by Von Kolnitz, and for values of $\frac{H}{B}$ of 1/5 to 1/12 and $\frac{L}{B}$ values of 1.3 to 3 by Johnson, Meyerhof equation fails to agree with the experimental results.

The modification, equation (33), derived for a closed jointed system along the same approach as of Meyerhof, thus also has the same defect of not taking the width of block into account, and thus the theoretical results obtained by using this equation does not agree with the experimental

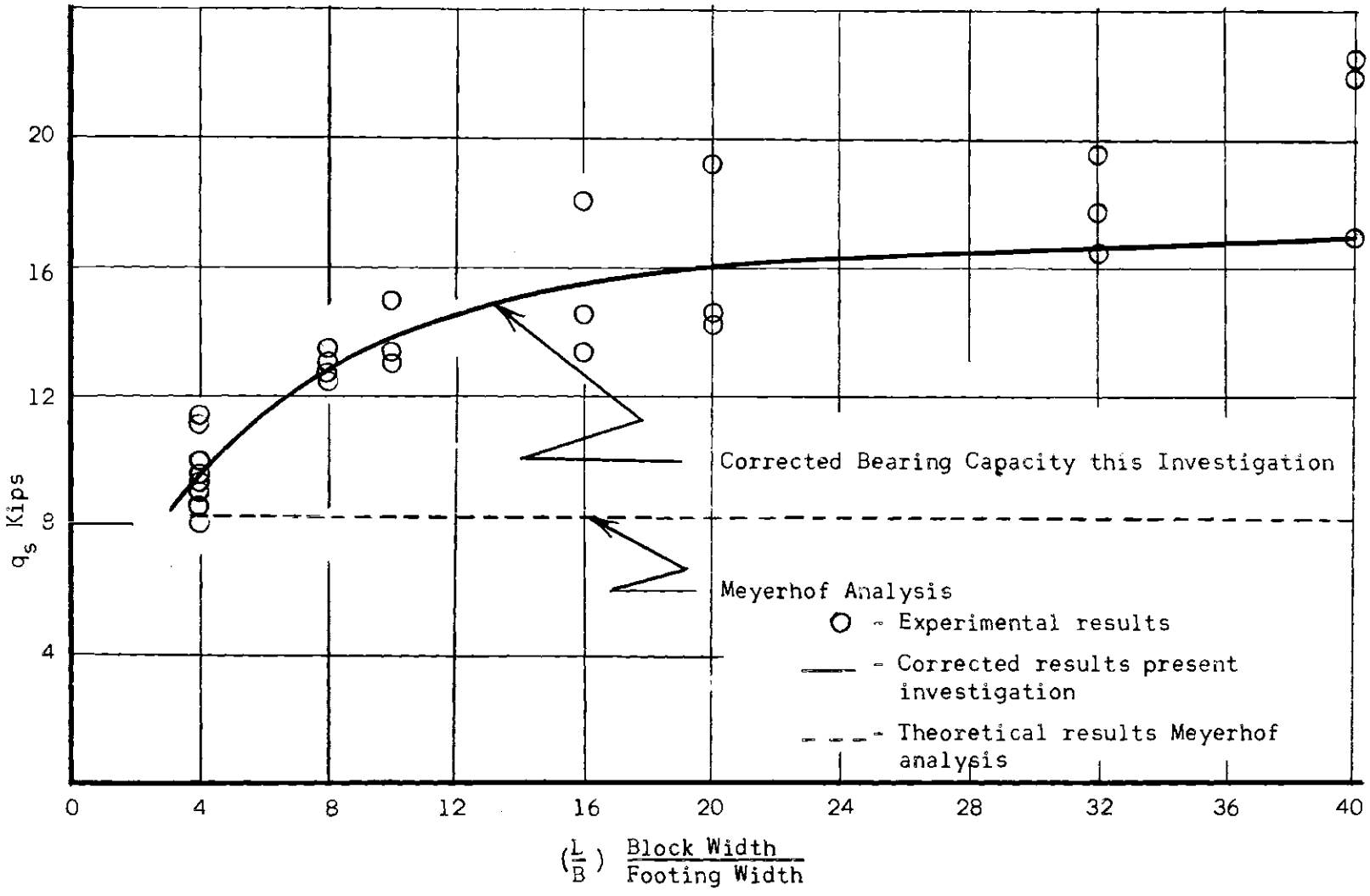

Figure 24. Bearing Capacity of Model Strip Footings on Open Jointed Rock.

results as shown in Table 7 and Table 24. Also in cases where $\frac{H}{B}$ value approaches the value of $\frac{\cot \alpha}{8}$ for the material, as in case of a 4" footing resting on a block of 1" thickness, the material having a φ value of 46°, according to Meyerhof's equation the bearing capacity becomes negative, which can never be the case, as Von Kolnitz tests on 4" width, 1" thick blocks of φ value 46° give positive bearing capacities. Thus it seems that Meyerhof's equation fails to explain many of the above mentioned defects.

Comparison with Von Kolnitz's Modification

Von Kolnitz suggested a modification of the Meyerhof equation. He suggested

$$q_{modified} = (q_o)(\frac{H}{B})$$

for the case of an open jointed system. This equation still fails to agree with the experimental results of this investigation where different block widths has been tested, Figure 26.

Von Kolnitz formula for square footings does not hold good, as, again it fails to take care of the width of the blocks. Also he used the expression given by Meyerhof for strip footings and modified it by $\frac{H}{B}$, which does not seem to work. He also stated that the modification only holds true where the footing width exceeds the thickness of rock. The equation was modified on only one series of tests on 1" block thickness and 4" width. Von Kolnitz did not vary the thickness or the width of the blocks in his investigation.

Comparison with Johnson Theory

Johnson in his investigation also showed that the modification

suggested by Von Kolnitz fails to agree with his experimental results. He also showed that the original Meyerhof equation, too, does not agree with his experimental results. Johnson performed a series of tests on rock blocks of size 4" x 4" x 1/4". He also used square footings in his investigation.

Johnson suggested another equation for the calculation of bearing capacity based on his experimental data. He represented the bearing capacity by a power function of the form

$$q_o = a\left(\frac{B}{L}\right)^n$$

in which the coefficient a is in psi units and n is a negative fractional unit.

His representation merely serves the purpose of showing the behavior of the bearing capacity with the ratio of footing width to block width. His expression cannot be used in any manner to find the bearing capacity of a jointed system, using the dimensions of the footing, block and the strength parameters of the rock material.

However, Johnson's investigation points out that the bearing capacity varies with the ratio of footing width to block width. Meyerhof's equation attempts to use the same formula for all blocks having ($L \geq H$). This seems to be the main cause of the difference in the results. As the present investigation also proves that increasing the block width, in case of a splitting failure, also increases the bearing capacity. Both the investigations done by Von Kolnitz and Johnson seem to be based on very limited amount of data, in the sense that the tests were done on only one size of blocks and no attempt was made to vary the thickness and width

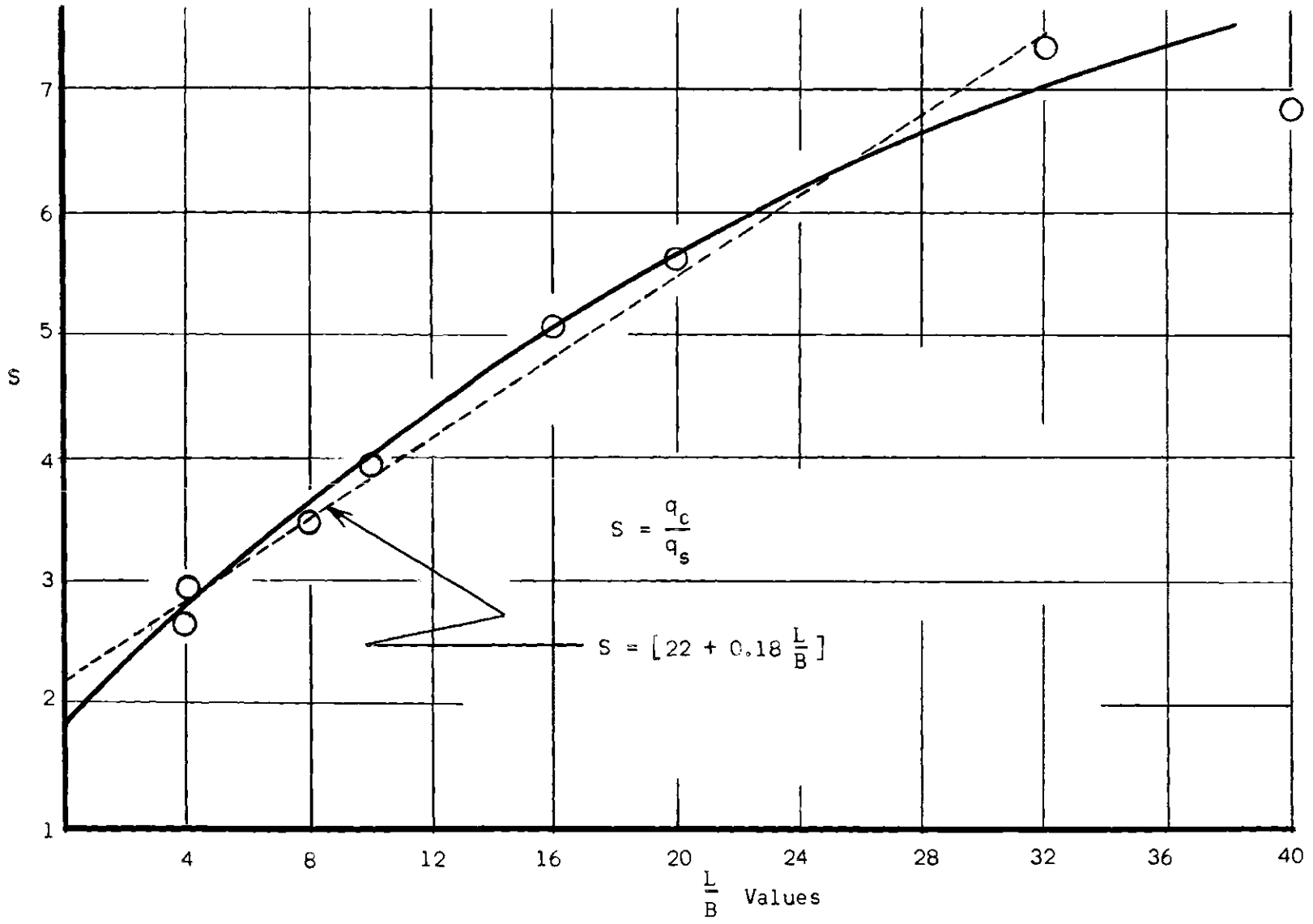

Figure 25. Variation of Factor S, i.e., Ratio of Bearing Capacity of Circular Footings to Experimental Bearing Capacity of Strip Footings with L/B Ratio.

of the blocks used. Thus the present investigation shows that all the previous equations suggested for the bearing capacity of open jointed systems or a block of rock in case of splitting failure cannot be used to give proper results.

Shape Factors

In an attempt to suggest a shape factor for the strip footings which could be used along with the equation developed in this investigation for the circular footings, the following method was used. The bearing capacity for a circular footing having same ratio of $\frac{H}{B}$ and $\frac{L}{B}$ as the strip footings was calculated by using equation (35).

The ratio S as the ratio of the theoretical bearing capacity of a circular footing having same $\frac{H}{B}$ and $\frac{L}{B}$ as that of the strip footing, to the experimental bearing capacity of strip footings used in this investigation was plotted against $\frac{L}{B}$ ratio for the strip footing. The plot is shown in Figure 25.

The graph shows the relation between $\frac{L}{B}$ and S. The curve up to $\frac{L}{B} = 32$ can be very closely approximated by a line. An emperical relation can be obtained between S and $\frac{L}{B}$ from this plot and S is given by

$$S = (2.2 + 0.18 \frac{L}{B}) \qquad (36)$$

$$= \frac{q_c}{q_s}$$

Thus by knowing the value of $\frac{L}{B}$ for the strip footing, the shape factor for the strip footing can be calculated from equation (36). Thus the bearing capacity of a strip footing up to $\frac{L}{B} = 32$ can be calculated by using the equation (35) and (36) and the bearing capacity is given by

$$q_s = \frac{J}{S}\left(cR_c + p_o R_p\right) \qquad (37)$$

$$= \frac{q_c}{s}$$

the values of J and S can be found by Equations (34) and (36) or by using the given charts for these factors in Figure 19 and Figure 25. However, the equation will give conservative results if used for values of $\frac{L}{B} > 32$.

The bearing capacity obtained by using equation (37) is given in Tables 6, 7 and 21 to 24, and shown in Figure 24 along with the experimental test results.

Tests were also conducted on square footings in this investigation. The results of the square footings are quite close to those of the circular footings. The variations are between 10 to 15 per cent of the results of circular footings. The bearing capacity of these square footings seems to be about 85 to 90 per cent of the bearing capacity of circular footings. Based on the experimental results, it is suggested to use a shape factor of 0.85 to 0.9 for the square footings resting on blocks of rock, or

$$q_{sq} = 0.85\ q_c$$

The results of the tests conducted on square footings are shown in Tables 8, 9, and 25 to 29, and in form of graph in Figure 26.

As stated earlier, the investigation is done on one type of rock. This was done keeping in mind the extensive number of tests required to take into account the changes in block length, width and height and the different footing shapes, in order to present quite a

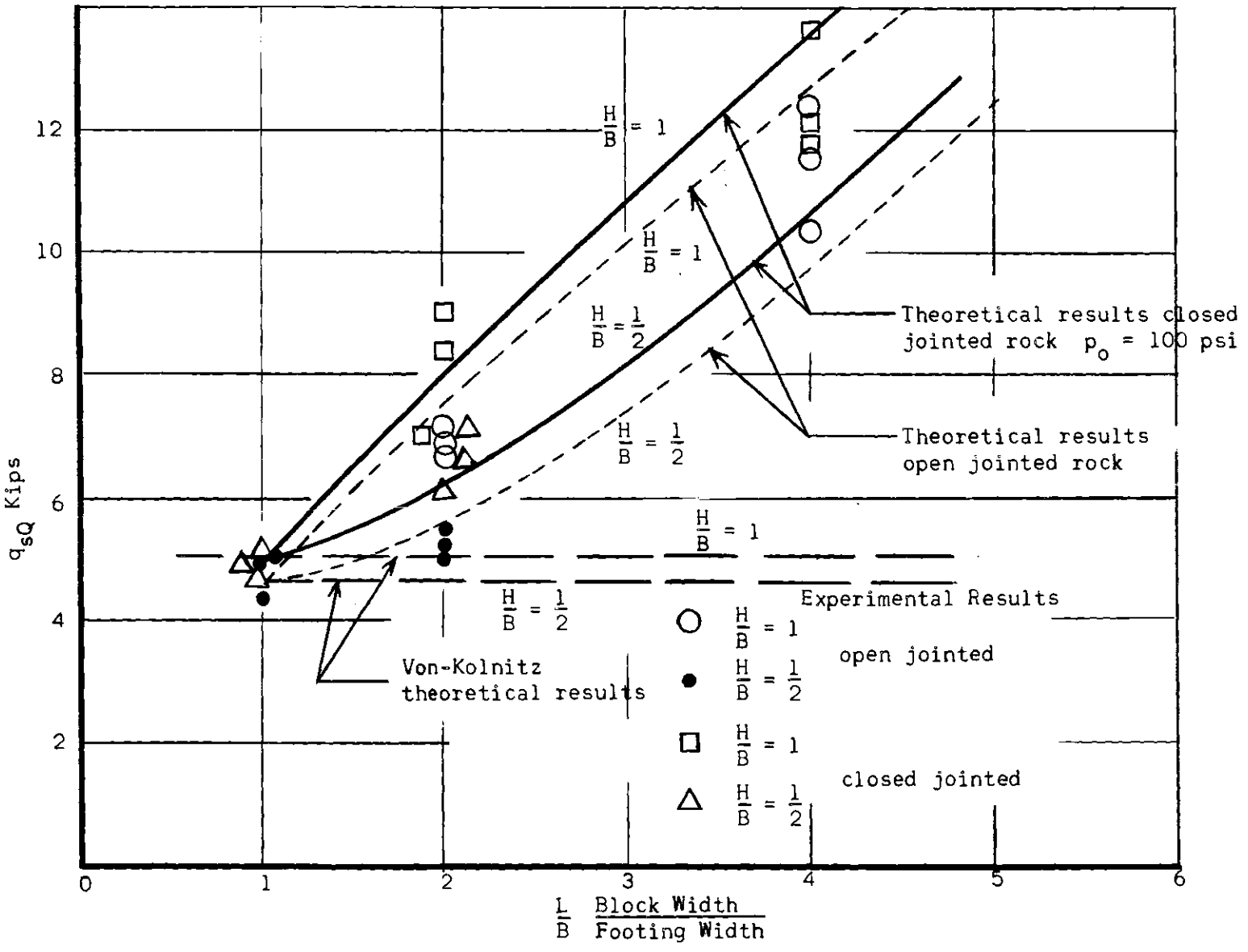

Figure 26. Bearing Capacity of Model Square Footings on Open and Closed Jointed Rock.

Table 8. Bearing Capacity Test Results for Square Footings on Open Jointed Rock System

Footing Size (In.)	L/B	H/B	Size of Blocks Width 4" Length 4" Thickness 1"												
			Experimental Q Lbs.				Experimental q (lbs./sq.in.)				Theoretical		Failure Settlement (Inches)		
			Q_1	Q_2	Q_3	$Q_{avg.}$	q_1	q_2	q_3	$q_{avg.}$	q_T	Q_T	S1	S2	S3
1	4	1	10,100	12,250	11,450	11,266	10,100	12,250	11,450	11,266	12,600	12,600	.03	.057	.048
2	2	1/2	19,800	21,700	20,600	20,700	4,950	5,425	5,150	5,175	5,650	22,600	.08	.092	.063
3	4/3	1/3	45,720	42,120	43,650	43,830	5,080	4,680	4,850	4,870	3,430	30,870	.069	.087	.048
4	1	1/4	68,500	76,200	72,260	72,320	4,281	4,762	4,516	4,520	4,610	73,760	.053	.097	.086

Table 9. Bearing Capacity Test Results for Square Footings on Closed Jointed Rock System, p_o = 100 psi

Footing Size (In.)	1/B	H/B	Size of Blocks Width 4" Length 4" Thickness 1"												
			Experimental Q Lbs.				Experimental q (lbs./sq.in.)				Theoretical		Failure Settlement (Inches)		
			Q_1	Q_2	Q_3	$Q_{avg.}$	q_1	q_2	q_3	$q_{avg.}$	q_T	Q_T	S1	S2	S3
1	4	1	11,800	13,650	12,050	12,500	11,800	13,650	12,050	12,500	13,450	13,450	.042	.068	.053
2	2	1/2	28,150	24,280	26,170	26,200	7,037	6,070	6,542	6,550	6,050	24,200	.075	.058	.093
3	4/3	1/3	52,100	45,300	47,320	48,240	5,788	5,033	5,258	5,360	3,680	33,120	.095	.086	.059
4	1	1/4	76,500	72,850	86,810	78,720	4,781	4,553	5,425	4,920	5,013	80,208	.065	.076	.086

comprehensive picture of the topic, which otherwise would not have been possible.

Applying the results of model footings to the prototype in the field involves dimensional analysis. The numerical value that is obtained by a test of a model depends on the values of the independent variables in the problem. A dimensional analysis of the relationship invariably leads to an equation, suggested by Buckingham, of the form

$$\pi = F(\pi_1, \pi_2, \ldots, \pi_p)$$

in which the π's are a complete set of dimensionless products. If we wish to know a particular value of π that corresponds to specified numerical values of $\pi_1, \pi_2, \ldots, \pi_p$, we may evidently achieve the result by means of a test of a model, provided that the independent dimensionless variables $\pi_1, \pi_2, \ldots, \pi_p$ have the same values for the model as for the prototype. The model and the prototype are then said to be completely similar. Since a complete set of dimensionless products determines all dimensionless products of the given variables, every dimensionless product has the same value for the model as for the prototype, when complete similarity exists. Obviously, complete similarity is impossible without geometric similarity.

Keeping this in view, the expressions or the deviations put forward in this investigation were brought in form of dimensionless ratios, so that a geometric similarity exists between the model and the prototype. The dimensional problem is very much reduced if two geometrically similar structures have similar loadings (in the sense that the loads on homologous parts have a constant ratio)(25). Thus having geometric similarity and

similar loadings the dimensional problem is only effected by smaller factors as time of loading, unit weight of material and the rate of loading.

The expressions suggested in this investigation are written in terms of φ and c, the strength parameters of the material, which are not affected by the scale, and will have the same value for the model and the prototype in the field. Thus, taking a suitable factor of safety, it appears that the results can be applied for the practical purposes. However, a detailed dimensional analysis will make some field tests also necessary to compare the results. The problem is similar to that for the soil bearing capacity, where with a suitable factor of safety, the theoretical results obtained through model studies have been applied in the field with success over the years.

The rock tested in this investigation, Indiana limestone, has almost isotropic properties, Mazanti (23), which may or may not be true for other rocks in the field. So the field rock should be tested in the direction of loading in the field for obtaining the φ and c values to be used in the expressions suggested in this investigation. The rock may also be tested in different directions and the least φ and c value can be used, which will give very safe, conservative, results.

At low confining pressures, some rock types are much more brittle than limestone. In particular, igneous rocks may be quite brittle because the silicate minerals resist plastic deformation much more than calcite. The expressions put forward in this investigation for the bearing capacity of jointed rock may not be applicable to the more brittle rock types. For more brittle rock types further investigation similar to this one will be

required before any conclusions can be given.

The joints of the rock may be filled with very soft matrix like clay in some cases in the field, in which case it will be safer to use it as an open jointed system, with no confinement on the loaded block. Also due to folds or stress history of the rock, there may be some confining pressures on the loaded block in the field. Thus, as is the case with most of the engineering problems in the field, a considerable amount of judgement will be required of the field engineer. However, it appears that choosing a suitable factor of safety, the expressions put forward in this investigation can be very well applied in the field.

Summary of Conclusions

The objectives of this investigation was to present some solution in form of expressions, which could be used to find the bearing capacity of rock blocks and jointed rock system for practical purposes. This investigation considers only vertical loads acting centrally on the loaded blocks of the jointed system

This investigation is confined to a single rock, with artificial jointing. The rock has almost isotropic and homogeneous properties. The results of this study can be applied to other rocks having similar properties as that of limestone and may not be applicable to other more brittle rock types. The bearing capacity of a closed jointed system is higher than that of the open jointed one.

As a result of this investigation, the following conclusions have been reached:

1. Meyerhof's equation for strip footings for splitting failure

and the equation modified along this line can only be applied for a limited range of rock block dimensions for $\frac{L}{B}$ about 4 and $\frac{H}{B}$ about 12 in which case the results by the above equations and the other equation suggested for strip footings in this investigation agree. For all other sizes of rock blocks, Meyerhof's equation cannot be applied.

2. For different sizes of rock blocks the expressions of Von Kolnitz and Johnson cannot be used. The expression suggested by Johnson shows the behavior of change in bearing capacity with the ratio of block width to footing size, but cannot be used to find the bearing capacity, knowing physical properties of the rock and the dimensions of footing and the rock block.

3. The bearing capacity of circular footings can be given by the following expression:

$$q_c = J(cR_c + p_o R_p)$$

where

$$R_p = \frac{2N_\varphi^2}{1 + N_\varphi} \left(\frac{L}{B}\right)^{(1 - \frac{1}{N_\varphi})}$$

$$R_c = (R_p - N_\varphi)\cot \varphi + 2N_\varphi^{1/2}$$

$$J = 0.53 \left(\frac{H}{B}\right)^{0.346} \quad \text{for } \frac{1}{2} \leq \frac{H}{B} \leq 8$$

and

$$J = 1 \quad \text{for } \frac{H}{B} > 8$$

For $\frac{H}{B}$ values of $\frac{1}{12}$ to $\frac{1}{2}$, the J value for $\frac{H}{B} = \frac{1}{2}$ can be used.

4. The bearing capacity of strip footings up to $\frac{L}{B} = 32$, can be represented by

$$q_s = \frac{J}{S} (cR_c + p_o R_p)$$

where

$$S = (2.2 + 0.18 \frac{L}{B})$$

5. The bearing capacity of square footings can be given by

$$q_{sq} = 0.85 \, J \, (cR_c + p_o R_p)$$

6. The Mohr φ angle of the material under plane strain conditions is about 7 per cent higher than the φ value under triaxial conditions where $\sigma_2 = \sigma_3$.

CHAPTER VIII

RECOMMENDATIONS FOR FURTHER STUDY

(1) Since this investigation is done on model footings and small sizes of rock blocks, it will be very useful if further study could be done on big blocks of rock or concrete using bigger footings, to look into the size effects, when using the results of model tests into the field.

(2) A study to examine the effects of another soft material, such as clay in the joints, can prove to be very useful, as such a system will be more close to the practical cases in the field.

(3) On this investigation only a system having horizontal and vertical joints have been studied. It will prove useful if studies could be done on another system having joints in different directions.

(4) Present investigation is done with footings resting in the middle of blocks or jointed systems, similar studies could be done changing the position of the footings on the block, and also footings centered over more than one block, or bridging one or more joints.

(5) Different more brittle rocks can be used to make a more comprehensive study with different shapes of footings to find shape factors and effects of different footing shapes on the rock bearing capacity.

APPENDIX

Table 10. Bearing Capacity Test Results for Circular Footings on Open Jointed Rock System

Footing Size (In.)	L/B	H/B	Size of Blocks Width 2" Length 2" Thickness 1" Experimental Q Lbs.				Experimental q (lbs./sq.in.)				Theoretical		Failure Settlement (Inches)		
			Q_1	Q_2	Q_3	$Q_{avg.}$	q_1	q_2	q_3	$q_{avg.}$	q_T	Q_T	S1	S2	S3
1	2	1	6,000	5,800	6,230	6,010	7,650	7,400	7,940	7,650	7,790	6,260	.035	.062	.042
2	1	1/2	18,500	14,800	12,450	15,250	5,890	4,710	3,970	4,850	4,610	14,500	.063	.040	.055

Table 11. Bearing Capacity Test Results for Circular Footings on Open Jointed Rock System

Footing Size (In.)	L/B	H/B	Size of Blocks Width 2" Length 2" Thickness 4" Experimental Q Lbs.				Experimental q (lbs./sq.in.)				Theoretical		Failure Settlement (Inches)		
			Q_1	Q_2	Q_3	$Q_{avg.}$	q_1	q_2	q_3	$q_{avg.}$	q_T	Q_T	S1	S2	S3
1	2	4	12,100 9,700	9,950 9,550	10,800 12,370	10,420 12,160	15,400	12,680	13,750	13,270	12,880	10,100	.056 .068	.043 .053	.067
2	1	2	16,100 15,440	15,200	17,500	16,060	5,130 4,920	4,840	5,570	5,110	4,610	14,500	.064 .046	.058	.035

Table 12. Bearing Capacity Test Results for Circular Footings on Open Jointed Rock System

Size of Blocks Width 4" Length 4" Thickness 4"

Footing Size (In.)	L/B	H/B	Experimental Q Lbs.				Experimental q (lbs./sq.in.)				Theoretical		Failure Settlement (Inches)		
			Q_1	Q_2	Q_3	$Q_{avg.}$	q_1	q_2	q_3	$q_{avg.}$	q_T	Q_T	S1	S2	S3
			21,200	20,800	18,750	19,400	27,000	26,400	23,850	24,680	22,600	17,780	.054	.068	.059
			19,600	17,400	20,200		25,000	22,180	25,750				.063	.071	.053
1	4	4	18,400	18,550	19,700		23,410	23,600	25,100				.087	.065	.044
			42,020	35,985	36,030	34,210	13,350	11,460	11,460	10,900	10,160	31,900	.083	.058	.067
2	2	2	33,980	23,015			10,820	7,330					.068	.073	

Table 13. Bearing Capacity Test Results for Circular Footings on Open Jointed Rock System

Size of Blocks
(1) Width 4" Length 4" Thickness 8"
(2) Width 4" Length 4" Thickness 16"
(3) Width 4" Length 4" Thickness 10"

Footing Size (In.)	L/B	H/B	Experimental Q Lbs.				Experimental q (lbs./sq.in.)				Theoretical		Failure Settlement (Inches)		
			Q_1	Q_2	Q_3	$Q_{avg.}$	q_1	q_2	q_3	$q_{avg.}$	q_T	Q_T	S1	S2	S3
1	4	8	21,650	20,400	19,450	20,500	27,600	26,000	24,800	26,120	26,410	20,800	.083	.042	.051
2	2	8	45,250	46,800	48,050	46,700	14,400	14,900	15,610	14,880	15,030	47,200	.061	.044	.057
1	4	10	19,650	21,600	21,900	21,050	25,000	27,500	27,900	26,800	26,410	20,800	.038	.043	.046
1	4	16	21,400	20,500	20,050	20,650	27,200	26,100	25,600	26,300	26,410	20,800	.044	.039	.042

Table 14. Bearing Capacity Test Results for Circular Footings on Open Jointed Rock System

Size of Blocks Width 8" Length 8" Thickness 4"

Footing Size (In.)	L/B	H/B	Experimental Q Lbs.				Experimental q (lbs./sq.in.)				Theoretical		Failure Settlement (Inches)		
			Q_1	Q_2	Q_3	$Q_{avg.}$	q_1	q_2	q_3	$q_{avg.}$	q_T	Q_T	S1	S2	S3
			33,200	32,800	33,900	32,335	42,300	41,800	43,200	41,200	38,900	30,500	.051	.046	.063
1	8	4	31,300	30,410	32,400		39,900	38,800	41,250				.048	.061	.056
			55,600	59,100	54,200		17,700	18,810	17,220				.035	.061	.048
			58,450	54,600	55,100	56,375	18,590	17,380	17,550	17,920	17,850	56,100	.063	.066	.054
2	4	2	56,600	57,350			17,990	18,250					.043	.058	

Table 15. Bearing Capacity Test Results for Circular Footings on Open Jointed Rock System

Footing Size (In.)	L/B	H/B	Size of Blocks Width 16" Length 16" Thickness 4"												
			Experimental Q Lbs.				Experimental q (lbs./sq.in.)				Theoretical		Failure Settlement (Inches		
			Q_1	Q_2	Q_3	$Q_{avg.}$	q_1	q_2	q_3	$q_{avg.}$	q_T	Q_T	S1	S2	S3
1	16	4	53,100	50,110	51,500	51,750	67,500	63,800	65,500	65,900	66,600	52,300	.046	.053	.068
2	8	2	88,600	93,300	95,600	92,500	28,220	29,700	30,400	29,420	30.620	96,400	.059	.039	.065

Table 16. Bearing Capacity Test Results for Circular Footings on Closed Jointed Rock System, P_o = 20 psi

Size of Blocks Width 4" Length 4" Thickness 1"

Footing Size (In.)	L/B	H/B	Experimental Q Lbs.				Experimental q (lbs./sq.in.)				Theoretical		Failure Settlement (Inches)		
			Q_1	Q_2	Q_3	$Q_{avg.}$	q_1	q_2	q_3	$q_{avg.}$	q_T	Q_T	S1	S2	S3
1	4	1	11,300	10,350	10,900	10,850	14,400	13,180	13,900	13,800	14,200	11,150	.050	.075	.068
2	2	1/2	19,000	22,500	20,750	20,750	6,050	7,020	6,600	6,600	6,350	19,950	.087	.040	.150
3	4/3	1/3	37,900	35,300	38,400	37,200	5,370	4,990	5,440	5,270	3,865	27,350	.130	.092	.083
4	1	1/4	62,800	57,300	67,700	62,600	5,000	4,570	5,390	4,990	4,690	59,000	.083	.108	.076

Table 17. Bearing Capacity Test Results for Circular Footings on Closed Jointed Rock System, P_o = 20 psi

Footing Size (In.)	L/B	H/B	Size of Blocks Width 2" Length 2" Thickness 1" Experimental Q Lbs.				Experimental q (lbs./sq.in.)				Theoretical		Failure Settlement (Inches)		
			Q_1	Q_2	Q_3	$Q_{avg.}$	q_1	q_2	q_3	$q_{avg.}$	q_T	Q_T	S1	S2	S3
1	2	1	5,400	7,000	6,980	6,460	6,880	8,920	8,880	8,240	8,090	6,350	.030	.080	.063
2	1	1/2	16,100	18,200	12,950	15,750	5,130	5,800	4,130	5,020	4,690	14,750	.062	.096	.087

Table 18. Bearing Capacity Test Results for Circular Footings on Closed Jointed Rock System, P_o = 100 psi

Footing Size (In.)	L/B	H/B	Size of Blocks Width 2" Length 2" Thickness 1" Experimental Q Lbs.				Experimental q (lbs./sq.in.)				Theoretical		Failure Settlement (Inches)		
			Q_1	Q_2	Q_3	$Q_{avg.}$	q_1	q_2	q_3	$q_{avg.}$	q_T	Q_T	S1	S2	S3
1	2	1	7,100	8,090	6,500	7,230	9,040	10,300	8,280	9,200	8,550	6,700	.091	.146	.083
2	1	1/2	18,000	16,700	16,450	17,050	5,740	5,320	5,240	5,430	5,013	15,750	.030	.057	.087

Table 19. Bearing Capacity Test Results on Circular Footings Tested in the Cell, p_o = 20 psi, Cell Pressure

Footing Size (In.)	L/B	H/B	Size of Blocks Width 4" Length 4" Thickness 1"												
			Experimental Q Lbs.				Experimental q (lbs./sq.in.)				Theoretical		Failure Settlement (Inches)		
			Q_1	Q_2	Q_3	$Q_{avg.}$	q_1	q_2	q_3	$q_{avg.}$	q_T	Q_T	S1	S2	S3
1	4	1	11,550	10,380	9,750	10,560	14,700	13,200	12,420	13,450	14,200	11,150	.086	.073	.058
2	2	1/2	22,930	19,300	22,570	21,600	7,290	6,145	7,170	6,880	6,350	19,950	.054	.078	.067
3	4/3	1/3	36,400	40,100	39,300	38,600	5,050	5,675	5,570	5,460	3,865	27,350	.064	.059	.083

Table 20. Bearing Capacity Test Results for Circular Footings Tested in the Cell, p_o = 100 psi, Cell Pressure

Footing Size (In.)	L/B	H/B	Size of Blocks Width 4" Length 4" Thickness 1"												
			Experimental Q Lbs.				Experimental q (lbs./sq.in.)				Theoretical		Failure Settlement (Inches)		
			Q_1	Q_2	Q_3	$Q_{avg.}$	q_1	q_2	q_3	$q_{avg.}$	q_T	Q_T	S1	S2	S3
1	4	1	12,150	11,020	9,740	10,970	15,450	14,060	12,400	13,960	14,950	11,730	.086	.094	.068
2	2	1/2	24,240	22,070	22,840	23,050	7,720	7,030	7,280	7,340	6,720	21,000	.038	.076	.083
3	4/3	1/3	40,800	39,260	38,140	39,400	5,790	5,550	5,380	5,580	4,090	35,800	.096	.084	.057

Table 21. Bearing Capacity Test Results for Strip Footings on Open Jointed Rock System, p_t = 420 psi

Size of Blocks (1) Width 1.4" Length 5" Thickness 4" (2) Width 2" Length 5" Thickness 4"

Footing Size (In.)	L/B	H/B	Experimental Q Lbs.				Experimental q (lbs./sq.in.)				Theoretical		Failure Settlement (Inches)		
			Q_1	Q_2	Q_3	$Q_{avg.}$	q_1	q_2	q_3	$q_{avg.}$	q_T	Q_T	S1	S2	S3
.35	4	11.5	15,900 14,100	17,200	15,700	15,725	9,140 8,010	9.820	8,980	8.980	8,510	9,440	.052 .032	.036	.032
.50	4	8	28,200 21,600	27,800	22,200	24,950	11,280 8,640	11,110	8,880	9,990	7,140	9,440	.032 .028	.042	.032

Table 22. Bearing Capacity Test Results for Strip Footings on Open Jointed Rock System, p_t = 420 psi

Size of Blocks (1) Width 7" Length 5" Thickness 4"
(2) Width 8" Length 5" Thickness 4"

Footing Size (In.)	L/B	H/B	Experimental Q Lbs.				Experimental q (lbs./sq.in.)				Theoretical		Failure Settlement (Inches)		
			Q_1	Q_2	Q_3	$Q_{avg.}$	q_1	q_2	q_3	$q_{avg.}$	q_T Meyerhof with S	Q_T	S1	S2	S3
.35	20	11.5	33,600	25,100	27,400	28,700	19,200	14,370	15,660	16,400	8,510	16,000	.073	.083	.066
.50	16	8	45,200	33,400	36,300	38,300	18,050	13,370	14,530	15,320	7,140	15,550	.085	.076	.058

Table 23. Bearing Capacity Test Results for Strip Footings on Open Jointed Rock System, p_t = 420 psi

Size of Blocks (1) Width 14" Length 5" Thickness 4"
(2) Width 16" Length 5" Thickness 4"

Footing Size (In.)	L/B	H/B	Experimental Q Lbs.				Experimental q (lbs./sq.in.)				Theoretical		Failure Settlement (Inches)		
			Q_1	Q_2	Q_3	$Q_{avg.}$	q_1	q_2	q_3	$q_{avg.}$	q_T	Q_T	S1	S2	S3
.35	40	11.5	38,300	42,700	39,300	40,100	21,850	24,390	22,420	22,950	8,510	16,950	.094	.076	.065
.50	32	8	48,800	41,200	44,400	44,800	19,530	16,460	17,750	17,930	7,140	16,550	.063	.087	.096

Table 24. Bearing Capacity Test Results for Strip Footings on Closed Jointed Rock System, P_o = 20 psi, p_t = 420 psi

Size of Blocks (1) Width 3.5" Length 5" Thickness 4" (2) Width 4" Length 5" Thickness 4"

Footing Size (In.)	L/B	H/B	Experimental Q Lbs.				Experimental q (lbs./sq.in.)				Theoretical		Failure Settlement (Inches)		
			Q_1	Q_2	Q_3	$Q_{avg.}$	q_1	q_2	q_3	$q_{avg.}$	q_T Meyerhof with S Modified	Q_T	S1	S2	S3
.35	10	11.5	24,600	28,300	22,400	25,100	14,050	16,150	12,800	14,330	8,703	14,030	.085	.078	.103
.50	8	8	30,150	33,600	38,400	34,050	12,050	13,430	15,370	13,620	7,264	12,970	.091	.065	.087

Table 25. Bearing Capacity Test Results for Square Footings on Open Jointed Rock System

Size of Blocks Width 2" Length 2" Thickness 1"

Footing Size (In.)	L/B	H/B	Experimental Q Lbs.				Experimental q (lbs./sq.in.)				Theoretical		Failure Settlement (Inches)		
			Q_1	Q_2	Q_3	$Q_{avg.}$	q_1	q_2	q_3	$q_{avg.}$	q_T	Q_T	S1	S2	S3
1	2	1	7,120	6,630	6,800	6,850	7,120	6,630	6,800	6,850	7,400	7,400	.042	.065	.084
2	1	1/2	17,300	18,950	20,390	18,880	4,325	4,962	5,097	4,720	4,610	18,440	.068	.054	.073

Table 26. Bearing Capacity Test Results for Square Footings on Open Jointed Rock System, p_t = 420 psi

(Johnson's Test Results)

Size of Blocks Width 4" Length 4" Thickness 1/4"

Footing Size (In.)	L/B	H/B	Experimental Q Lbs				Experimental q (lbs./sq.in.)				Theoretical		Failure Settlement (Inches)		
			Q_1	Q_2	Q_3	$Q_{avg.}$	q_1	q_2	q_3	$q_{avg.}$	q_T	Q_T	S1	S2	S3
1 1/4	3.2	1/5	10,740	10,820	10,280	10,610	6,880	6,940	6,560	6,810	8,200	12,800			
2	2	1/8	18,700	20,000	20,700	19,800	4,670	5,000	5,710	4,950	4,960	19,840			
3	4/3	1/12	34,200	40,000	41,000	38,400	3,800	4,450	4,560	4,270	3,200	28,800		.084	.082
4	1	1/16	56,000	57,100	54,800	56,000	3,500	3,560	3,420	3,500	3,980	63,680	.165	.134	.107

Table 27. Bearing Capacity Test Results for Square Footings on Closed Jointed Rock System, P_o = 20 psi

Size of Blocks Width 4" Length 4" Thickness 1"

Footing Size (In.)	L/B	H/B	Experimental Q Lbs.				Experimental q (lbs./sq.in.)				Theoretical		Failure Settlement (Inches)		
			Q_1	Q_2	Q_3	$Q_{avg.}$	q_1	q_2	q_3	$q_{avg.}$	q_T	Q_T	S1	S2	S3
1	4	1	12,800	11,650	10,950	11,800	12,800	11,650	10,950	11,800	12,780	.068	.073	.085	
2	2	1/2	22,650	25,040	23,950	23,880	5,662	6,260	5,987	5,970	5,720	22,880	.076	.053	.047
3	4/3	1/3	48,350	42,850	44,475	45,225	5,372	4,761	4,942	5,025	3,480	30,320	.053	.087	.069
4	1	1/4	73,800	78,200	81,280	77,760	4,612	4,887	5,080	4,860	4,690	75,040	.056	.083	.091

Table 28. Bearing Capacity Test Results for Square Footings on Closed Jointed Rock System, p_o = 20 psi

Footing Size (In.)	L/B	H/B	Size of Blocks Width 2" Length 2" Thickness 1" Experimental Q Lbs.				Experimental q (lbs./sq.in.)				Theoretical		Failure Settlement (Inches)		
			Q_1	Q_2	Q_3	$Q_{avg.}$	q_1	q_2	q_3	$q_{avg.}$	q_T	Q_T	S1	S2	S3
1	2	1	7,050	6,800	7,270	7,040	7,050	6,800	7,270	7,040	7,280	7,280	.046	.057	.081
2	1	1/2	20,600	19,740	17,380	19,240	5,150	4,935	4,345	4,810	4,690	18,760	.065	.074	.053

Table 29. Bearing Capacity Test Results for Square Footings on Closed Jointed Rock System, p_o = 100 psi

Footing Size (In.)	L/B	H/B	Size of Blocks Width 2" Length 2" Thickness 1" Experimental Q Lbs.				Experimental q (lbs./sq.in.)				Theoretical		Failure Settlement (Inches		
			Q_1	Q_2	Q_3	Q_{avg}	q_1	q_2	q_3	$q_{avg.}$	q_T	Q_T	S1	S2	S3
1	2	1	9,040	8,400	7,010	8,150	9,040	8,400	7,010	8,150	7,700	7,700	.065	.044	.061
2	1	1/2	20,500	18,600	19,460	19,520	5,125	4,650	4,865	4,880	5,013	20,052	.054	.087	.049

BIBLIOGRAPHY

1. Klaus, John W., "An Approach to Rock Mechanics," Journal of the Proceedings of the A.S.C.E., Soil Mechanics and Foundations Div., Aug. 1962, pp. 1-29.

2. Meyerhof, G. G., "The Bearing Capacity of Concrete and Rock," Magazine of Concrete Research, April, 1953.

3. Meyerhof, G. G., "The Ultimate Bearing Capacity of Foundations," Geotechnique, Vol. II, No. 4, December, 1951.

4. Feda, J., "Research on Bearing Capacity of Loose Soil," Proceedings Fifth International Conference on Soil Mechanics and Foundation Engineering, Vol. 1, pp. 635, 1961.

5. Pauker, H. E., "An Explanatory Report on the Project of a Sea Battery," Journal of the Ministry of Ways and Communications, Sept., 1889.

6. Rankine, W. J. M., A Manual of Applied Mechanics, London, Charles and Griffin Co., 1953.

7. Ritter, M., "Limits of Equilibrium of Earths and Loose Materials," International Association Bridge and Structures, 1936.

8. Bell, A. L. by A. W. Skempton, "Arthur Laugtry Bell and His Contributions to Soil Mechanics," Geotech. Vol. 8, No. 4, 1958.

9. Prandtl, L. "Uber die Harte plastischer Korper, Nachrichten von der Koniglichen Gesellschaft der Wissenschaften zu Gottingen" Mathematisch-physikalische Klasse aus dem Jahre 1920, Berlin, pp. 74-85, 1920.

10. Terzaghi, K., Theoretical Soil Mechanics, John Wiley and Sons, Inc., New York, 1943.

11. Bach, C., and Baumann, R., Elastizitat und Festigkeit, Berlin, J. Springer Verlag, p. 217, 1924.

12. Graf, O., "Uber einige Aufgaben der Eisenbetonforschung aus alterer und neuerer Zeit," Beton und Eisen, Vol. 33, No. 11, pp. 165-173, June, 1934.

13. Hensen, B., "The Bearing Capacity of Sand, Tested by Loading Circular Plates," Proc. Fifth Int. Conf. Soil Mech., pp. 659.

14. Sokolovski, V. V., Statics of Granular Media, Pergamon Press, Oxford, London, 1965.

15. Hajal, "Etude Generale de la Butee d'un Ecran plan Contre un Massif Coherent par la Theorie des Caracteristiques," Thesis, Fluid Mechanics Laboratory, University of Grenoble, France, 1961.

16. Lundgren, H., and Mortensen, "Determination by Theory of Plasticity, the Bearing Capacity of Continuous Footings on Sand," Proc. Third Int. Conf. Soil Mech., 1, pp. 409.

17. De Beer, E. E., and Ladanyi, B., "Etude Experimentale de la Capacite portante du Sable Sous des Foundations Grunlarees Etables en Surface," Proc. Fifth Int. Conf. Soil Mech., 557, 1961.

18. Bauschinger, J., "Versuche mit Quadern aus Natursteinen," Munich, Mitteilungen aus dem Mechanischtechnischen Laboratorium der Kgl. Technischen Hochschule, No. 7, p. 13, 1876.

19. Sowers, G. B., "Load Required to Compress Concrete and Rock," Engineers' Notebook, Civil Engineering, August 1943.

20. Von Kolnitz, George F., "An Investigation of the Bearing Capacity of a Jointed Rock System," MS Thesis, Georgia Institute of Technology, September, 1965.

21. Johnson, A. C., "Bearing Capacity of a Thin Layered Jointed Rock System," MS Thesis, Georgia Institute of Technology, April, 1966.

22. Schwartz, A. E., "An Investigation of the Strength of Rock," Ph.D. Thesis, Georgia Institute of Technology, May, 1963.

23. Mazanti, B. B., "The Effect of the Intermediate Principal Stress on the Strength of Rock," Ph.D. Thesis, Georgia Institute of Technology, June, 1967.

24. Sachs, G., and J. D. Lubahn, "Strength of Cylindrical Dies," Journal of Applied Mechanics, Vol. 10, pp. A-147 - A-155, 1943.

25. Langhaar, H. L. Dimensional Analysis and Theory of Models, John Wiley and Sons, Inc., New York, 1951.

26. Meyerhof, G. G., "The Bearing Capacity and Consolidation of Soils and Settlement of Foundations," Master's Thesis, University of London, 1943.

27. Hoffman and Sachs, Introduction to Theory of Plasticity for Engineers, McGraw-Hill Book Company, Inc., New York, 1953.

Other References

1. Meyerhof, G. G., "An Investigation of the Bearing Capacity of Shallow Footings on Dry Sand," Proceedings, Second International Conference Soil Mechanics. 1, 237.

2. Nadai, A., Theory of Flow and Fracture of Solids, Vol. 1, McGraw-Hill Book Company, Inc., New York, 1950.

3. Jurgenson, L., "The Application of Theories of Plasticity and Elasticity to Foundation Problems," "Contributions to Soil Mechanics 1925-1940," Journal of Boston Society of Civil Engineers, Boston, 1934.

4. Mizuno, T., "On the Bearing Power of Soil under a Uniformly Distributed Circular Load," Third Int. Conf. Soil Mech., pp. 446, 1953.

5. Meyerhof, G. G., "Shallow Foundations," A.S.C.E. Journal of Soil Mechanics Foundation Division, Vol. 91, SM2, pp. 21, March, 1965.

6. Hill, R., The Mathematical Theory of Plasticity, Oxford at the Clarendon Press, 1950.

7. Button, S. J., "The Bearing Capacity of Footings on a Two Layer Cohesive Sub-Soil," Proc. Third Int. Conf. Soil Mech., Vol. 1, p. 332.

8. Drucker, D. C., and Prager, W., "Soil Mechanics and Plastic Analysis or Limit Design," Quarterly Journal of Applied Mathematics, 10, 157, 1952.

9. Biarez, J., and Baurel, M., Wack, B., "Contribution a l'etude de la force portante des foundations," Proc. Fifth Int. Conf. Soil Mech., Vol. 1, p. 603, 1961.

10. Jumikis, A. R., "The Shape of Rupture Surface in Dry Sand," Proc. Fifth Int. Conf. Soil Mech., p. 693.

11. Malyshev, M. V., Fjedorov, I. V., "Plastic and Elastic Plastic Problems in the Design of Foundations," Proc. Fifth Int. Conf. Soil Mech., Vol. 1, pp. 727.

12. Milovic, D. M., "Comparison Between the Calculated and Experimental Values of the Ultimate Bearing Capacity," Proc. Sixth Int. Conf. Soil Mech., Vol. 2, pp. 142.

13. Balla, A., "Bearing Capacity of Foundations," Journal Soil Mech. Found. Div., Proc. AM Soc. of C.E., 1962.

VITA

Banwari Lal Bishnoi was born August 20, 1939 in Haripura (Punjab), India. He graduated from MBM Engineering College at Jodhpur, India in 1961. For two years, he worked as a Junior Engineer on the Rajasthan Canal project. He received a Master of Technology in Civil Engineering from Indian Institute of Technology, Bombay, in 1965 and joined Georgia Institute of Technology in Atlanta, Georgia, in the fall of the same year.